Energy, Mines and Resources Canada
Earth Physics Branch
1 Observatory Crescent
Ottawa Canada
K1A 0Y3

Énergie, Mines et Ressources Canada
Direction de la physique du globe
1 Place de l'Observatoire
Ottawa Canada
K1A 0Y3

Geomagnetic Service of Canada

Service géomagnétique du Canada

MAGNETO-TELLURIC SURVEY OF THE MOUNT MEAGER REGION OF THE SQUAMISH VALLEY

(British Columbia)

Pham Van Ngoc

77 pps. comprenant 46 figures

Dossier public de la Direction de la physique du globe No. 80-8-E
Earth Physics Branch Open File Number 80-8-E
Ottawa, Canada

Contract Series No:
No. de séries du contrat:
OsQ79 - 00045

Ministère de l'Energie, des Mines et des Ressources du Canada
Département de Physique du Globe
Division de Géomagnétisme

Department of Energy, Mines and Resources Canada
Earth Physics Branch
Division of Geomagnetism

Price/Prix: $21.50

RESUME

La présente étude magnéto-tellurique (M.T.) a été effectuée dans deux périmètres différents de la chaîne côtière de la Colombie britannique.

L'étude de la région du Mont Meager fait suite à deux autres campagnes effectuées en 1976 et en 1977. A la différence des deux campagnes précédentes, la présente étude couvre principalement les parties hautes du Mont Meager.

Le deuxième périmètre est situé dans la haute vallée de la rivière Squamish, à l'ouest du Mont Cayley.

A cause du relief important rencontré notamment dans la région du Mont Meager, on a étudié l'effet théorique de la topographie par des modèles numériques à deux dimensions. L'examen des résultats théoriques et expérimentaux permet de conclure que l'influence de la topographie n'est pas négligeable surtout pour la polarisation H, mais que l'influence prédominante sur les résultats M.T. reste celle des structures profondes, notamment pour la polarisation E.

Les résultats de la présente campagne M.T. dans la région du Mont Meager, complétant ceux des campagnes précédentes, ont permis de mettre en évidence l'existence, sous le volcan, d'une zone très conductrice, dont le toit se situerait seulement à 2 km sous le niveau de la mer. La forte conductivité électrique de cette zone pourrait être liée à la présence d'une chambre magmatique bordée par deux accidents tectoniques majeurs à l'Est et au Nord du volcan.

Dans la vallée de Squamish, les résultats semblent indiquer aussi l'existence d'une zone conductrice profonde, bornée, de 20 km de largeur environ, encadrant le Mont Cayley. Le toit de cette zone se situerait vers 6 km de profondeur sur la bordure Ouest, et à plus de 12 km au Sud.

L'existence des zones conductrices situées à des profondeurs relativement faibles, sous les deux régions volcaniques étudiées, concorde avec les gradients géothermiques élevés trouvés dans ces régions et confirme par conséquent leur grand intérêt pour la géothermie.

SUPPLY AND SERVICES CANADA
Ottawa, Ontario.

IREM-MERI
Montreal, Quebec

Contract series No: OSQ79-00045

Department of Energy, Mines & Resources Canada
Earth Physics Section
Geomagnetic Division

MAGNETO-TELLURIC SURVEY OF THE MOUNT MEAGER REGION OF THE SQUAMISH VALLEY (BRITISH COLUMBIA)

by

PHAM VAN NGOC

February 1980

MAGNETO-TELLURIC SURVEY OF THE MOUNT MEAGER REGION AND THE SQUAMISH VALLEY

(British Columbia)

INDEX

SUMMARY

A magnetotelluric (M.T.) survey was made in two different areas of the coastal range of British Columbia.

The Mount Meager survey is the follow-up of two other surveys made in 1976 and 1977. The present survey covers the higher regions of Mount Meager.

The second perimeter is located in the upper valley of the Squamish River, west of Mount Cayley.

Due to the rugged topography, especially in the Mount Meager area, the theoretical effect of topography has been studied with two-dimensional models. Theoretical and experimental results show that topographic effects are significant especially for H polarisation, but the dominant influence on M.T. results is the one due to deep structures, especially for E polarisation.

The results of the present M.T. survey in the Mount Meager area complete those of previous years and show the existence of a highly conductive zone under the volcano. The top of this zone is only 2 km below sea level. The high electric conductivity of this zone could be due to the presence of a magmatic chamber, confined by two major tectonic folds east and north of the volcano.

In the Squamish River valley around Mount Cayley, results tend to indicate the existence of a deep confined conductive zone, about 20 km wide. The top of this zone is about 6 km deep on the west side and over 12 km deep to the south.

The existence of conductive zones at relatively shallow depth, below the two volcanic zones studied, matches the high geothermal

gradients found in these regions and confirms their considerable significance as geothermal sources.

MAGNETO-TELLURIC SURVEY OF THE MOUNT MEAGER REGION AND THE SQUAMISH VALLEY (British Columbia)

1. INTRODUCTION

The magneto-telluric (M.T.) survey described in this paper was carried out in two different perimeters of the coastal chain of British Columbia; one in the Mount Meager region, the other in the Squamish Valley near Mount Cayley. Mount Meager and Mount Cayley are two quaternary volcanoes, forming part of the Garibaldi volcanic chain, which has a general north-south direction. A number of geological surveys (Souther, J.G., 1975; Lewis, T.J. and Souther, J.G., 1978) have shown the existence of a significant geothermic potential in these two regions. Temperature measurements in drill holes have shown geothermal gradients approximately twice the normal gradient (Lewis, J.F., 1978).

The measurements at Mount Meager were made following two other M.T. surveys; one in 1976 in the Lillooet Valley to the east of Mount Meager and one in 1977 where the sites prospected were along one part of the Lillooet River and up the valley to the north of Mount Meager, as well as Meager Creek to the east and south of the volcano. Unlike the two preceding surveys, the present study concentrates on the upper parts of Mount Meager, which have a rugged relief. In addition to the practical difficulties in setting up measuring stations, there is a considerable topographic effect which will be considered later before the interpretation of the results in this region.

The second perimeter, situated in the upper valley of the Squamish River, to the west of Mount Cayley, was surveyed by M.T. for the first time. This present study is thus of a reconnaissance nature.

2 - GEOGRAPHICAL LOCATION

In the Mount Meager region, the stations are only accessible by helicopter. Four stations were set up according to the terms of the contract, however, only station ME.3 could be placed in the location specified. The three other proposed station locations were situated in zones having a great deal of snow, and thus had to be moved elsewhere. Station ME.4 was moved approximately 1.5 km towards the southwest and station ME.1 2.5 km towards the south. The suggested location of ME.2 was situated close to Mount Meager, and it was absolutely impossible to find another convenient location in the immediate region. After several fruitless attempts to find a suitable location, this station was placed in a different sector situated about 4 km to the west of station ME.4 (see Figure 1).

The stations in the Squamish Valley are accessible by car. However, in the perimeters studied, the valley is relatively narrow, and, aside from logging roads, there is very little access. The forest in this area is extremely dense and inaccessible to ordinary vehicles. It was not possible to find six stations uniformly distributed over all the perimeter studied. Four were placed in the north part of the valley and two in the south part (see Figure 2). Table I gives the U.T.M. coordinates of the group of ten stations set up in the two perimeters.

TABLE I

U.T.M. Coordinates of the ten stations.

Station	Longitude	Latitude
ME.1	466,650 mE	5,605,600 mN
ME.2	457,750	5,603,150
ME.3	457,900	5,611,300
ME.4	462,050	5,603,500
SQ.1	473,100	5,550,150
SQ.2	471,900	5,551,050
SQ.3	471,600	5,552,400
SQ.4	470,300	5,550,900
SQ.5	475,600	5,546,075
SQ.6	475,800	5,544,850

3 - APPARATUS AND DATA PROCESSING

The apparatus as well as the method of data processing was described in the first report (Pham Van Ngoc, 1976). The M.T. profiling instrument (P.M.T.), the TELMAG2, measures the apparent scalar resistivity following the direction of the telluric line placed on the ground for twelve discrete frequencies from 1 to 2000 Hz. The M.T. probe line simultaneously records two telluric components and two magnetic components, both sets of which are horizontal and orthogonal. This data is subsequently processed to obtain the two principal directions as well as the corresponding tensor apparent resistivities which are designated respectively $\rho_{a_{12}}$ and $\rho_{a_{21}}$.

4 - THE TOPOGRAPHIC EFFECT

Using M.T., it is possible to calculate the effect of two-dimensional structures of any form by different numeric methods. In this way, C.C. Ku (1973) used the electric network analogy method to calculate the topographic effect of a number of individual models.

We have used the same method to study the topographic effect of three two-dimensional models, having the form and dimensions close to that of the reliefs encountered in the Mount Meager region and in the Squamish Valley. These are: a hill, a valley, and a slope, whose M.T. anomalies are shown respectively in Figures 3, 4, and 5. Each model follows a profile perpendicular to the extension of the relief, and the curves represent the variation of the two principal apparent resistivities, corresponding respectively to the E (E//) polarisation and the H (//), for two resistivities of rocks and for two different frequencies.

From an examination of the results obtained for these three models we may make the following comments:

4.1 H Polarisation: The topographic effect is important principally where there is a break in the slope, as well as at the top of a hill and at the bottom of a valley. At mid-slope, the effect may be completely negligible. Another interesting characteristic of the H// anomalies is their small variation with frequency. As a consequence, the topographic effect has very little influence at a given station on the M.T. probe curve corresponding to H//, except for the change in the resistivity value of the rocks which make up the relief.

4.2 E Polarisation: In all cases, the topographic effect is much smaller than for H//. It is more important at the high frequencies, but very rapidly becomes negligible for low frequencies.

From this study, we may conclude that the topographic effects can be avoided by using the results corresponding to E//. In the case being considered, especially as it concerns the Mount Meager stations, which were generally located at mid-slope (see Figure 1), we estimate that the topographic effects should not substantially modify the M.T. results. For the stations in the Squamish Valley, the topographic effect may introduce a slight anisotropy through a systematic increase in the apparent resistivities corresponding to H//. We will see further on, however, that the M.T. sounding curves in the Squamish Valley do not show such an effect. The same is true of the data taken during the preceding surveys in the Lillooet Valley.

5 - MOUNT MEAGER REGION

The figures numbered from 6 to 9 correspond respectively to the four stations ME.1, ME.2, ME.3 and ME.4 in the Mount Meager region. These figures show the curves of the tensor apparent resistivities obtained in the two principal directions designated respectively $\rho_{a_{12}}$ and $\rho_{a_{21}}$. The principal directions are also shown, on the same figures, by the lines with arrowheads at each end. The solid lines correspond to $\rho_{a_{12}}$ and the dotted lines to $\rho_{a_{21}}$. The orientation angles of the lines are indicated with respect to the northern geographic directions (N.G.). The principal directions are given only for three periods (10^{-2}, 1 and 25 seconds) in the range studied, since they change very little from one period to another. When the apparent resistivities are isotropic in a given period, we use the symbol ρ_a.

The direction $\rho_{a_{12}}$ is close to the NS geographic direction and $\rho_{a_{21}}$ is close to the geographical EW. For the sake of convenience, the following nomenclature will be used:

$$\rho_{a_{12}} \approx \rho_a^{NS}$$

$$\rho_{a_{21}} \approx \rho_a^{EW} \quad .$$

5.1 Topographic Effect

Before any interpretation, we will first consider the possible influence of topography on the results obtained at the four stations ME.1-ME.4 placed in the heavily-folded relief of the Mount Meager region.

Station ME.1. This station may be considered to be placed at the top of an elongated hill stretching in the EW direction (see Figure 1). From the theoretical results of Figure 3, we have

$$\rho_a NS(H//) < \rho_a EW(E//) \quad .$$

From Figure 6, we see that:

$$\rho_{a_{12}}(NS) < \rho_{a_{21}}(EW) \quad .$$

Thus the anisotropy observed at station ME.1 may arise from the topographic effect. However, we also note from Figure 6 that the anisotropy becomes accentuated at the lower frequencies in going from 100 Hz to 1 Hz. This is in contradiction to the theoretical results of Figure 3. In conclusion, the topographic effect of station ME.1 may have a certain influence towards the higher frequencies (>100 Hz), but this influence is small compared to that of deep structures.

Station ME.2. The topography at this station is close to that of a hill in the NS direction. As a result:

$$\rho_a EW(H//) < \rho_a NS(E//) \quad .$$

From Figure 7, we have:

$$\rho_{a_{21}}(EW) > \rho_{a_{12}}(NS) \quad .$$

Thus, the topographic effect is not predominant at station ME.2.

Station ME.3. The hill at this station is in the SW-NE direction. From Figure 8, we note that this direction is close to that of $\rho_{a_{21}}$. Thus from the theoretical results, we have:

$$\rho_{a_{12}}(H//) < \rho_{a_{21}}(E//) \ .$$

This is shown in Figure 8, and the same comments apply as those made on station ME.1.

Station ME.4. The topography is complex around this station (see Figure 1). As a first approximation, we may consider the station as placed on the upper half of a slope going in the EW direction. From the theoretical results of figure 5:

$$\rho_a NS(H//) < \rho_a EW(E//) \ .$$

From Figure 9, we have:

$$\rho_{a_{12}}(NS) < \rho_{a_{21}}(EW)$$

for frequencies greater than 5 Hz. However the anisotropy is reversed for the very low frequencies. The topography may have an influence at high frequencies but not at low frequencies.

In the present survey, the fact that the sites studied are situated in the high parts of Mount Meager, may give rise to some doubt as to the importance of the topographic effect. The theoretical results given in paragraph 4 confirm this importance, especially for H polarisation. However, an examination of the experimental results at the four stations ME.1-ME.4, leads us to conclude that the real topographic effect is not as important as the theoretical effect, since the theoretical models assume breakpoints which are too abrupt, and also assume an indefinite extension in one direction. Their cylindrical form acts to accentuate the topographic effect corresponding to H polarisation.

The topographic effect is certainly not negligible, but may introduce distortions at the higher frequencies. At low frequencies, it definitely seems that the influence of deep structures is predominant.

5.2 Qualitative Interpretation

The results are first examined qualitatively before addressing the problem of quantitative interpretation.

Figures 6 to 9 show that stations ME.1 and ME.4, situated at the southern part of the volcano, to the south of Mount Meager, exhibit a very strong electrical anisotropy. This is not the case at station ME.3 situated to the NW, above Mosaic Creek, where the anisotropy arises only from superficial structures (up to a period of 1 second). At station ME.2, placed away from the volcano to the SW, the apparent resistivities are practically isotropic. Evidently the recent quaternary volcanic rocks are electrically anisotropic, at least in the superficial part, while the old volcanic rocks are more isotropic.

Figures 10 and 11 provide a summary of the results from the four Mount Meager stations respectively along the two principal directions, NS and EW. In Figure 10, corresponding to the NS direction, ME.1, ME.3 and ME.4 have a similar aspect, while ME.2 shows a different form. The apparent resistivities $\rho_{a_{12}}$ are larger at ME.2, especially for the short periods. This again confirms the difference in the electrical properties of old volcanic rocks and recent rocks. The recent rocks are more conducting in their superficial part, due almost certainly to a higher porosity. The apparent resistivities $\rho_{a_{21}}$ along

the EW direction (see Figure 11) have the same aspect for the four stations, but the values at ME.4 are noticeably smaller for the long periods.

Table II below gives the cylindrical skew coefficient for the four stations in the three frequency ranges used.

TABLE II

Mount Meager - Skew Values

Stations	100 - 1 Hz	1 - 0.1 Hz	0.1 - 0.01 Hz
ME.1	0.2 - 0.5	0.6 - 0.8	0.8
ME.2	0.6 - 0.8	0 - 0.3	0.3 - 0.6
ME.3	0 - 0.2	0.7 - 1	0.6 - 1
ME.4	0 - 0.3	0.2 - 0.6	0.2 - 0.4

ME.1 and ME.4 have a small skew, except for ME.1 at low frequencies. The highest values of skew at ME.2 can be explained by the absence of a well-identified anisotropy. The same holds for ME.3 in the low frequency ranges.

In the following sections, the results are given in the form of maps, including those obtained during the 1977 survey (Pham Van Ngoc, 1978), around Mount Meager, in order to provide a more complete structural picture of the volcano.

5.2.1 Maps of the principal directions and the principal apparent resistivities at frequency F = 100 Hz (Figs. 12, 13 and 14)

Figure 12 shows the presence of a marked change in the principal directions for the four stations ME.1-ME.4. This is due

to a structural heterogeneity in the superficial part of the volcano. Nevertheless, ME.1 and ME.4 exhibit a continuity with stations SH.2 and SH.1 respectively from the 1977 survey.

The maps of the apparent resistivities $\rho_{a_{12}}$ and $\rho_{a_{21}}$ in Figures 13 and 14 confirm the existence of a general lowering of the resistivity in the interior of the volcano, which was detected during the 1977 survey. The present maps provide a better definition of the conducting zones. We note especially two zones of minimum resistivity, one situated in the southern part and the other to the NW of Mount Meager.

5.2.2 Maps of the principal directions and principal apparent resistivities at frequency F = 1 Hz (Figures 15, 16 and 17)

The map of the principal directions (Figure 15) shows that the rocks tend to become isotropic at greater depths to the west of Mount Meager. The conducting zone at the interior of the volcano tends to extend along a general SE-NW direction with a move towards the NNE direction in the southern part (see Figures 16 and 17). The existence of two conducting axes which converge towards the south of Mount Meager is particularly evident on the map $\rho_{a_{21}}$ (EW) in Figure 17 and is confirmed by the principal directions.

5.2.3 Maps of the principal directions and principal apparent resistivities at frequency F = 0.04 Hz (Figures 18, 19 and 20

The maps of the principal apparent resistivities (Figures 19 and 20) show only a single conducting zone at considerable depth, with a tendency to extension in the SE-NW direction. Nevertheless this

zone is not cylindrical and has an irregular shape. This is evident from the irregular orientations of the principal direction particularly to the south of Mount Meager (see Figure 18).

5.3 Quantitative Interpretation

5.3.1 Choice of principal direction

From the maps of principal apparent resistivities and principal directions show above, we can obtain an overview of the complexity of the internal structure of the Mount Meager volcano, as well as its deep structure. A quantitative interpretation would be difficult since the overall structure of the volcano can only be conveniently represented by a three-dimensional model.

Nevertheless, we will attempt the best approximation possible, by closely re-examining the characteristics of the sounding curves from the four stations ME.1-ME.4. As was mentioned previously, stations ME.1 and ME.4 show a very strong electrical anisotropy (see Figures 6 and 9) since they are located in the southern part of Mount Meager where the structural complexity, particularly in the superficial zones, was emphasized in the preceding report (Pham Van Ngoc, 1978, Figure 37). However the maps of the principal apparent resistivities at frequency F = 1 Hz reveal locally conducting axes which are close to the NS direction (see Figures 16 and 17). The tabular approximation would thus be better using the longitudinal apparent resistivities $\rho_{a_{12}}$(NS).

Station ME.2 shows a weak anisotropy (see Figure 7). Nevertheless, the choice of $\rho_{a_{12}}$(NS) appears more appropriate, if only to avoid the topographic effect in this region.

Station ME.3 shows an apparent anisotropy only at the high frequencies (see Figure 8). In addition, all the maps of apparent resistivities examined above clearly indicate a lengthening of the conducting zone in the SE-NW direction. The choice of $\rho_{a_{12}}$ is the best one here since it corresponds to this direction of lengthening.

To sum up, for the four stations studied in the Mount Meager region, the tabular approximation is better for interpretation of the sounding curves corresponding to $\rho_{a_{12}}$(NS). The results of this interpretation are shown in Figures 21-24 corresponding to the four stations ME.1-ME.4. For comparison, we have also interpreted the four curves corresponding to $\rho_{a_{21}}$(EW) and these results are shown in Figures 25-28.

5.3.2 Geoelectric cross-sections along two profiles

To have a better idea of the results obtained, they have been presented in the form of a geoelectric cross-section along two profiles in the NW-SE direction (see Figure 30). Profile 1 uses station ME.3 and station SH.2 from the 1977 survey, passing near the summit of Mount Meager. Profile 2 is situated more to the south, including also station SH.1 from the 1977 survey. The two geoelectric cross-sections obtained in this way are shown in Figure 29. Recalling that the results obtained for the four stations ME.1-ME.4 of the present survey correspond to $\rho_{a_{12}}$(NS) for the reasons outlined above, we note that the same holds for SH.2. Only the results of SH.1 correspond to $\rho_{a_{21}}$(EW) for the reasons already cited in the previous report (Pham Van Ngoc, 1978; paragraph 7.3).

Figure 29 shows the existence of a deep conducting layer that is continuous according to profile 1, and whose top should be situated between 2 and 4 km depth only. From profile 2, the conducting layer is discontinuous between ME.2 and ME.4 and its top is deeper, going to 7-8 km.

5.3.3 Map of the isobaths of the top of the deep conducting layer

The existence of a deep conducting layer had already been established during the two preceding surveys, even in the zones outside of the Mount Meager region. They are significant for geothermal considerations, and constitute the principal objectives of the M.T. studies carried out in the region.

We have thus attempted to fill out the isobath map of the top of the deep conducting layer under Mount Meager and its immediate vicinity, using the results of the two last M.T. surveys (see Figure 30). The contours, drawn every 2 km, indicate the absolute altitude of the top with respect to sea level.

For reasons already set out, the quantitative results should be used with caution because of the tabular approximation, which, although it has both a theoretical and experimental justification, cannot provide an absolute exact value. Nevertheless, they give a good indication in relative values and provide a general picture of the structure and of the deep tectonic. In this regard, Figure 30 provides very interesting information. Firstly, it shows the existence, under Mount Meager, of a very conductive zone, in the form of an anticlinal whose top may reach a height of 2 km under sea level. The low resistivity

of this conducting zone, as low as 4 Ωm, can only be explained by the high porosity and the high content of electrolyte, along with the existence of an elevated temperature at a shallow depth. If we assume an electrolyte having a NaCl concentration equivalent to about 0.1 molar, Archimedes Law provides an estimate of the porosity of the conducting zone that may be as high as 20% and a geothermal gradient that could be of the order of 120° per km. From this we may assume the existence of melted rocks at 10 km depth at least, in the form of a magmatic chamber under Mount Meager. Using this hypothesis, Figure 30 shows that the magmatic chamber is bordered on the east and the north by two major tectonic folds which separate the internal zone of the volcano from the external zone, where the depth of the top of the conducting layer decreases abruptly up to 18 km which is the order of magnitude of the thickness of the terrestrial crust found in the Lillooet valley. The west and south borders of the volcano are less clear through lack of data.

6 - THE SQUAMISH VALLEY

The figures numbered 31 to 36 correspond respectively to the six stations ST.1-ST.6 in the Squamish Valley. The presentation format of the tensor apparent resistivity curves is the same as that used for the curves from Mount Meager.

The Squamish Valley is relatively narrow and we would anticipate a topographic effect like the one shown in Figure 4. However, as in the case of Mount Meager, a detailed examination of the results from the six stations ST.1-ST.6 leads to the same conclusion, that the influence of deep structures is still predominant, in the M.T. sounding curves in the Squamish Valley.

6.1 Qualitative Interpretation

Stations ST.1, ST.2 and ST.3, in the northern part of the valley, have resistivities which are practically isotropic at high frequencies (>1 Hz). The topographic effect would thus appear to be negligible. The anisotropy is only evident for low frequencies, and is small. The corresponding principal directions are very close to the NS and EW geographic directions (see Figures 31, 32 and 33).

Station SQ.4, situated more to the west in the Elaho Valley, shows a stronger anisotropy. The apparent resistivities there are also generally larger due to the fact that in this location there are none of the more conducting glacial deposits which are found in the Squamish Valley. The inclination of the principal directions may be caused by the relief, which is more folded in this area.

Stations SQ.5 and SQ.6 are positioned in the southern part of the valley near Turbid Creek. The anisotropy there is more pronounced, but it may be caused by the topographic effect since:

$$\rho_{a_{12}}(\text{NS}) > \rho_{a_{21}}(\text{EW})$$

while from the theoretical results of Figure 4, we should have the reverse.

Figure 37 shows the 6 curves of the apparent resistivity $\rho_{a_{12}}$ in the NS direction. We note a very marked resemblance between SQ.1, SQ.2 and SQ.3 on one hand, and SQ.5 and SQ.6 on the other. Station SQ.4, however, for reasons already noted, is different from the other stations. Conversely, in Figure 38 which contains the 6

curves corresponding to $\rho_{a_{21}}$(EW), we observe that these last curves have the same general features and that they crease strongly at the low frequencies.

Table III, below, gives the skew for the six stations in the Squamish Valley.

TABLE III

Squamish Valley - Skew Values

Station	100 - 1 Hz	1 - 0.1 Hz	0.1 - 0.001 Hz
SQ.1	0 - 0.4	0 - 0.2	0.3 - 0.7
SQ.2	0.5 - 0.8	0.5 - 0.8	0.2 - 0.8
SQ.3	0 - 0.2	0.5 - 0.8	0.3 - 0.8
SQ.4	0 - 0.2	0 - 0.3	0.2 - 0.4
SQ.5	0.4 - 0.8	0 - 0.2	0 - 0.4
SQ.6	0 - 0.4	0.6 - 0.8	0.3 - 0.6

Generally speaking, the skew shows no features which are out of the ordinary, which leads us to expect a structural complexity. Nevertheless, the existence of an anisotropy in two dimensions in the Squamish Valley is probable, the two principal directions of the anisotropy being approximately oriented along the NS and EW geographic directions.

6.2 Quantitative Interpretation

To provide an explanation for the observed anisotropy, we have numerically calculated the theoretical effect of an infinitely long conducting cylinder, having a rectangular cross-section 20x10 km, with the top surface placed at 6 km depth. Referring to Figure 39,

we see that the two curves corresponding respectively to E// and H// diverge at the low frequencies, which is the anisotropic effect created by a conductive cylinder. The appearance of the curves E// and H// resembles that from stations SQ.1, SQ.2 and SQ.3. By way of comparison, Figure 39 shows the curves for $\rho_{a_{12}}$ and $\rho_{a_{21}}$ from station SQ.2. The correspondence between the two curves is not perfect, but the effect is similar. The model presented may constitute a possible hypothesis for interpretation of the results. In Figure 39, we also show the curve T corresponding to a tabular structure of 3 terrains with an intermediate conductive layer which has the same thickness as the height of the conductive cylinder. We note that the descending branch of curve E// coincides largely with that of the curve T, but rises sooner towards the low frequencies. As a consequence, if we interpret the curve E// as resulting from a tabular structure, we will obtain a thickness of the conducting layer which is smaller or a larger resistivity than in the cylindrical case. Conversely, the depth of the top of the cylinder may be obtained with good accuracy by the tabular approximation of the E// curve. These points lead us to interpret only the $\rho_{a_{12}}$(NS) curves whose results are given in Figures 40-45 corresponding respectively to the six stations SQ.1-SQ.6.

The results of the interpretation of stations SQ.1, SQ.2 and SQ.3, show that the top of the conductive layer is situated about 6 km deep. Its average resistivity, of the order of 90 Ωm, is probably too high. The actual resistivity should be less than this value.

At stations SQ.5 and SQ.6, the depth of the top is greater, of the order of 12 km. The resistivity of the conductive layer is also higher, around 340 Ωm. The actual resistivity should also be lower.

The curve $\rho_{a_{12}}$ of station SQ.4 is complicated. A 7-terrain model must be used to interpret it. However, these results do not appear very significant because of a non-negligible influence of the relief which is very folded and complex in this location.

6.3 Discussion of the results

As we have already emphasized in the introduction, the present M.T. survey in the Squamish Valley is a reconnaissance survey. In the project, we expected to place the stations only along the logging roads. Because this road follows the NS direction of the valley, it did not provide a good distribution of the stations to give the best study of the relation between the structure of the deep tectonic and another quaternary volcano in the Garibaldi chain in the NS direction: Mount Cayley.

We have seen, in the preceding paragraph, that the deep structure of Mount Meager, situated more to the north, is also complex. It was possible to propose a structural diagram which allows an explanation of the anomalies, thanks to a better distribution of stations around Mount Meager. However, the quasi-totality of the stations there is accessible only by helicopter.

It is thus difficult with the stations presently available in the Squamish Valley to propose an adequate structural diagram for this perimeter. In spite of a certain homogeneity of the results between the stations SQ.1, SQ.2 and SQ.3 on the one hand, and SQ.5 and SQ.6 on the other, there is an important difference between these two groups, without considering the unorthodox behaviour of SQ.4.

Nevertheless, a possible hypothesis has been proposed above to explain the results. This hypothesis assumes the existence of a deep conductive zone, limited in extent, and about 20 km wide. This is plausible knowing the overall tectonic related to the formation of the quaternary Garibaldi volcanic chain. Figure 46 shows, schematically, the location of this zone, which should probably include Mount Cayley. In the immediate vicinity of this volcano, the top of the conducting zone is situated about 6 km deep, according to the results obtained from stations SQ.1, SQ.2 and SQ.3. Similar results were also obtained at Mount Meager.

The depth of the conducting zone up to 12 km at stations SQ.5 and SQ.6, may be caused by a major tectonic fold in the EW direction to the south of Mount Cayley. This fold would be the origin of the observed anisotropy in the sounding curves from SQ.5 and SQ.6, especially at average and high frequencies. As to SQ.4, the anomalies in SQ.4 can only be explained by parasitic effects of the relief or from complexities in the superficial structures.

Temperature measurement in two drillholes situated near sations SQ.1 and SQ.3, show a geothermal gradient of the order of $60^{\circ}C/km$ (Lewis, J.F., 1978). At a depth of 6 km, the temperature would be about $360^{\circ}C$. At this temperature, a rock with 5% porosity containing electrolyte having a concentration equivalent to 0.1 molar NaCl, would have a resistivity of the order of 70 Ωm. This is approximately the figure observed for resistivity in the conductive zone under SQ.1, SQ.2 and SQ.3.

7 - GENERAL CONCLUSIONS AND RECOMMENDATIONS

The study of the topographic effect during the present survey has established that its influence is not as important as had been thought. Even if it can give rise to local perturbations in severe conditions, the predominant influence on the M.T. results remain due to deep structures. This study emphasizes the possibility of using M.T. in an investigation of structure and of deep tectonics in mountainous areas which are of significant interest for both economic and scientific reasons.

The results of the present survey in the region of Mont Meager, complete those done during preceding surveys, and provide a better understanding of the deep structure of this quaternary volcano situated in the extreme north of the Garibaldi chain. Certainly the results given should not be regarded as definitive, given the inherent structural complexity of volcanoes, and the relatively small number of stations set up in these regions such as these which are very difficult to access. In spite of this, the M.T. results have provided evidence of the existence of a very hot zone situated a few km deep under Mount Meager, whose origin may be related to the existence of a magmatic chamber. These results confirm the considerable geothermic interest in this volcano.

In the Squamish Valley, the present study can only provide a rough interpretation. A simplistic structural diagram has been proposed and remains to be verified.

The influence of topography, if not negligible, is at least not predominant, and this leads us to recommend a more comprehensive setting up of M.T. stations, in the high regions as well as in the

neighboring valleys around Mount Meager, in order to better confirm the existence of the magmatic chamber, and to establish its extent especially in the south and west border. The same recommendation holds for Mount Cayley where the deep structure is very poorly understood.

Pham Van Ngoc

Geophysical Engineer, Doctorate in Science,
Montreal, 30 January 1980

REFERENCES

KU C.C., HSIEH M.S. and LIM S.H. (1973)
The Topographic Effect in Electromagnetic Fields.
Canad. J. Earth Sci., v. 10, no. 5, p. 645-656.

LEWIS J.F. (1978)
Preliminary Field Report of Drilling Near Mount Meager and Mount Cayley Volcanic Centres. 1977
EMR, Earth Phys. Br., Open File Rep. 78-1, Ottawa.

LEWIS T.J. and SOUTHER J.G. (1978)
Meager Mountain, B.C. - A Possible Geothermal Energy Resource.
EMR, Earth Phys. Br., Geothermal Ser., no. 9, Ottawa.

PHAM VAN NGOC (1976)
Magneto-telluric Reconnaissance Survey in the Lillooet Valley, B.C.
IREM-MERI Rep. 1976, Montreal.
EMR, Earth Phys. Br., Open File 77-20, Ottawa.

PHAM VAN NGOC (1978)
Magneto-telluric Prospecting in the Mount Meager Geothermal Region.
IREM-MERI Rep. 1978, Montreal.

SOUTHER J.G. (1975)
Geothermal Potential of Western Canada.
In Proc. Sd. U.N. Symps. on the Development and Use of Geothermal Resource, Vol. 1, p. 259-267.

LIST OF FIGURES

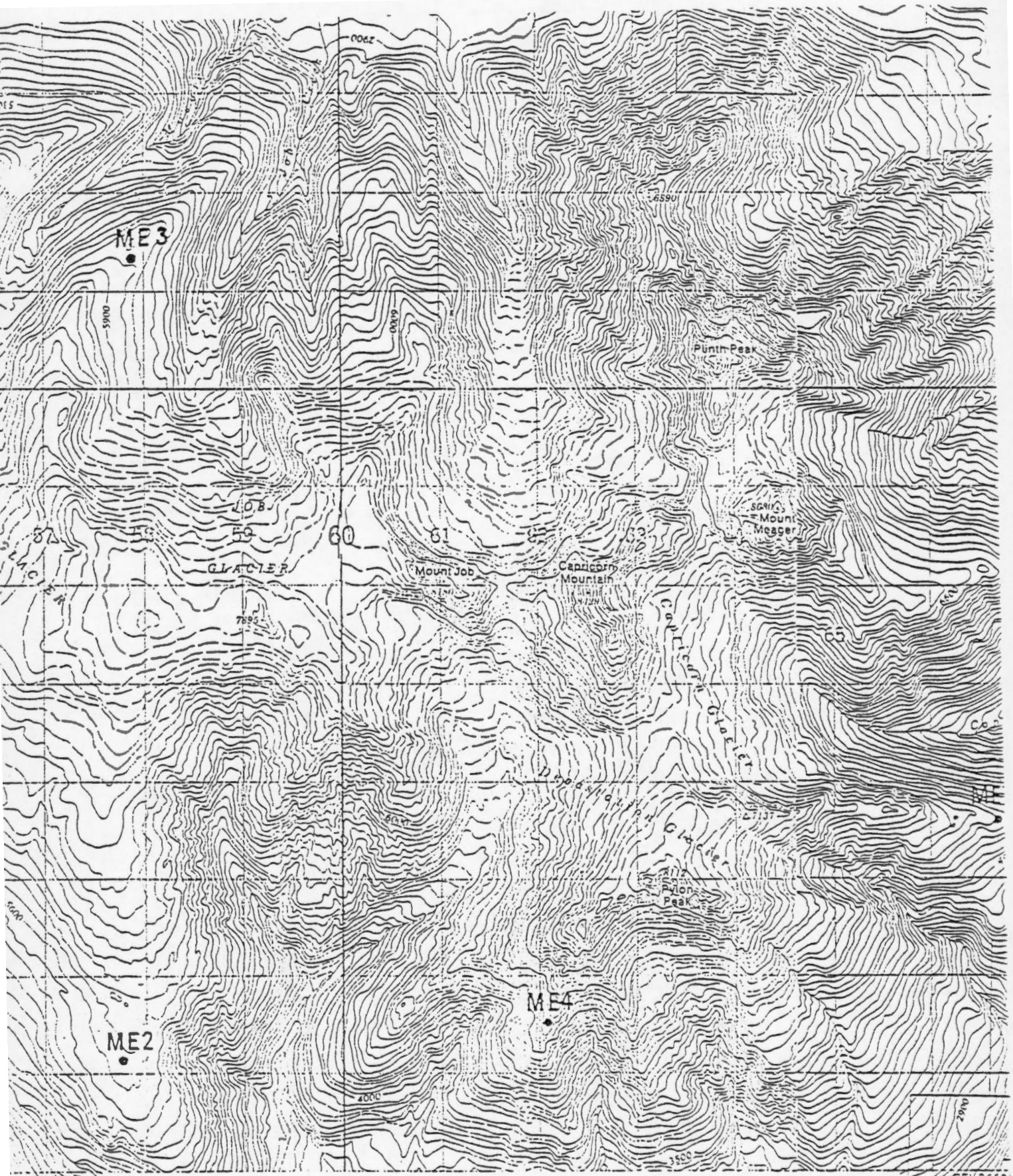

Figure 1 Région du Mont Meager. Situation géographique des sites de mesure: ME1, ME2, ME3, ME4.
Meager Mountain region. Geographical location of measure sites: ME1, ME2, ME3, ME4.

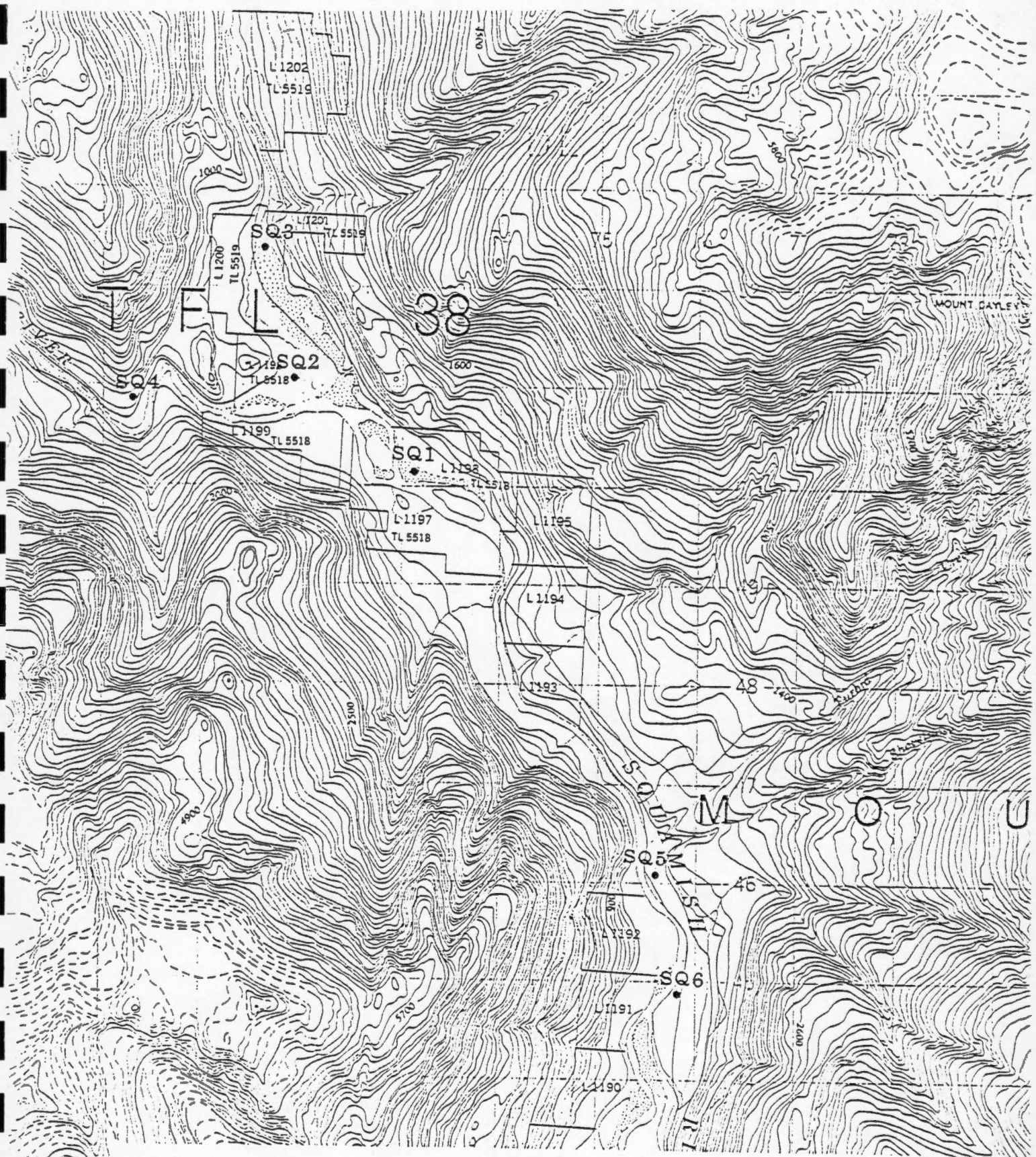

Figure 2 Vallée de Squamish. Situation géographique des sites de mesure: SQ1, SQ2, SQ3, SQ4, SQ5, SQ6.
Squamish Valley. Geographical location of measure sites: SQ1, SQ2, SQ3 , SQ4, SQ5, SQ6.

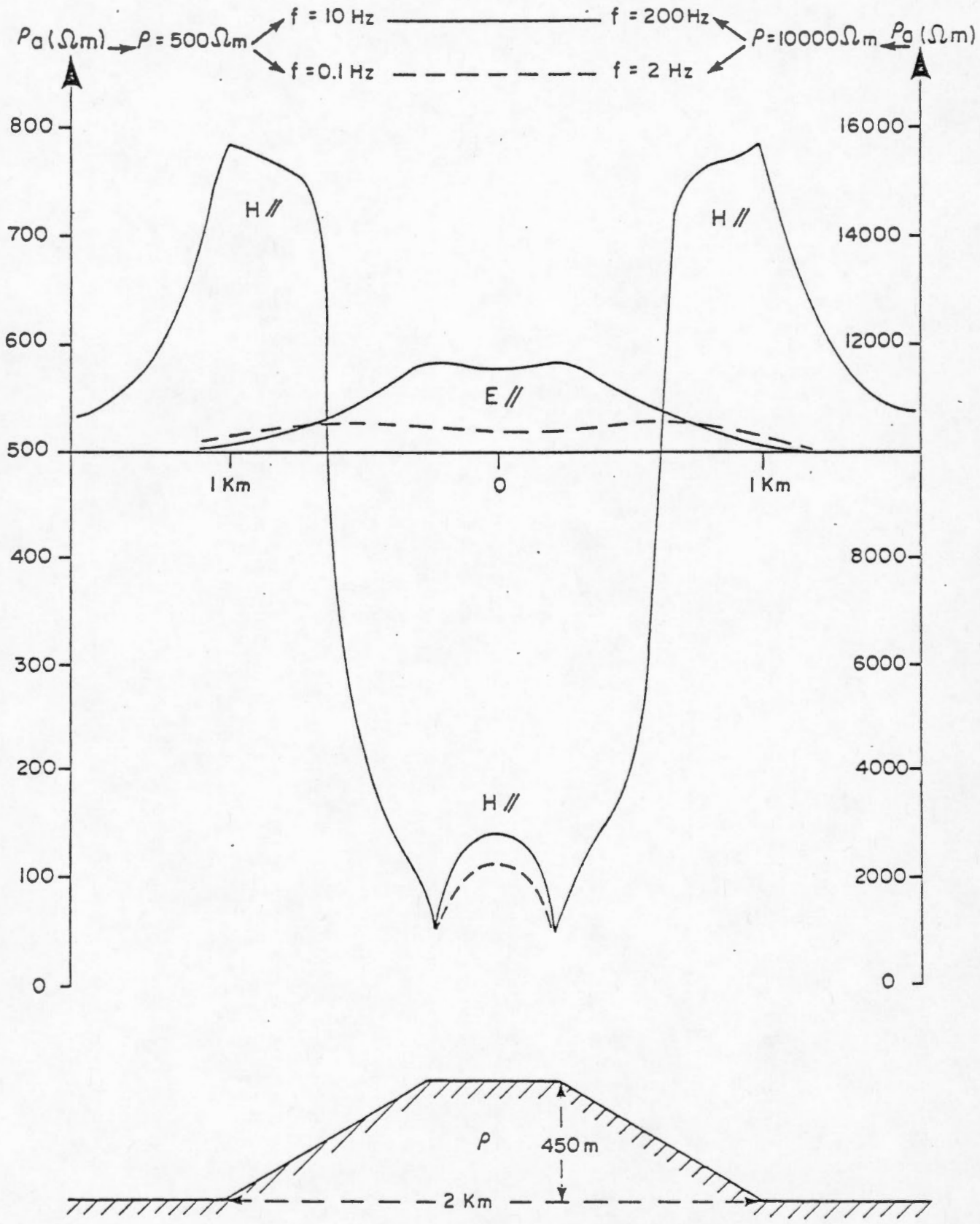

FIGURE 3. Effet topographique d'une colline.

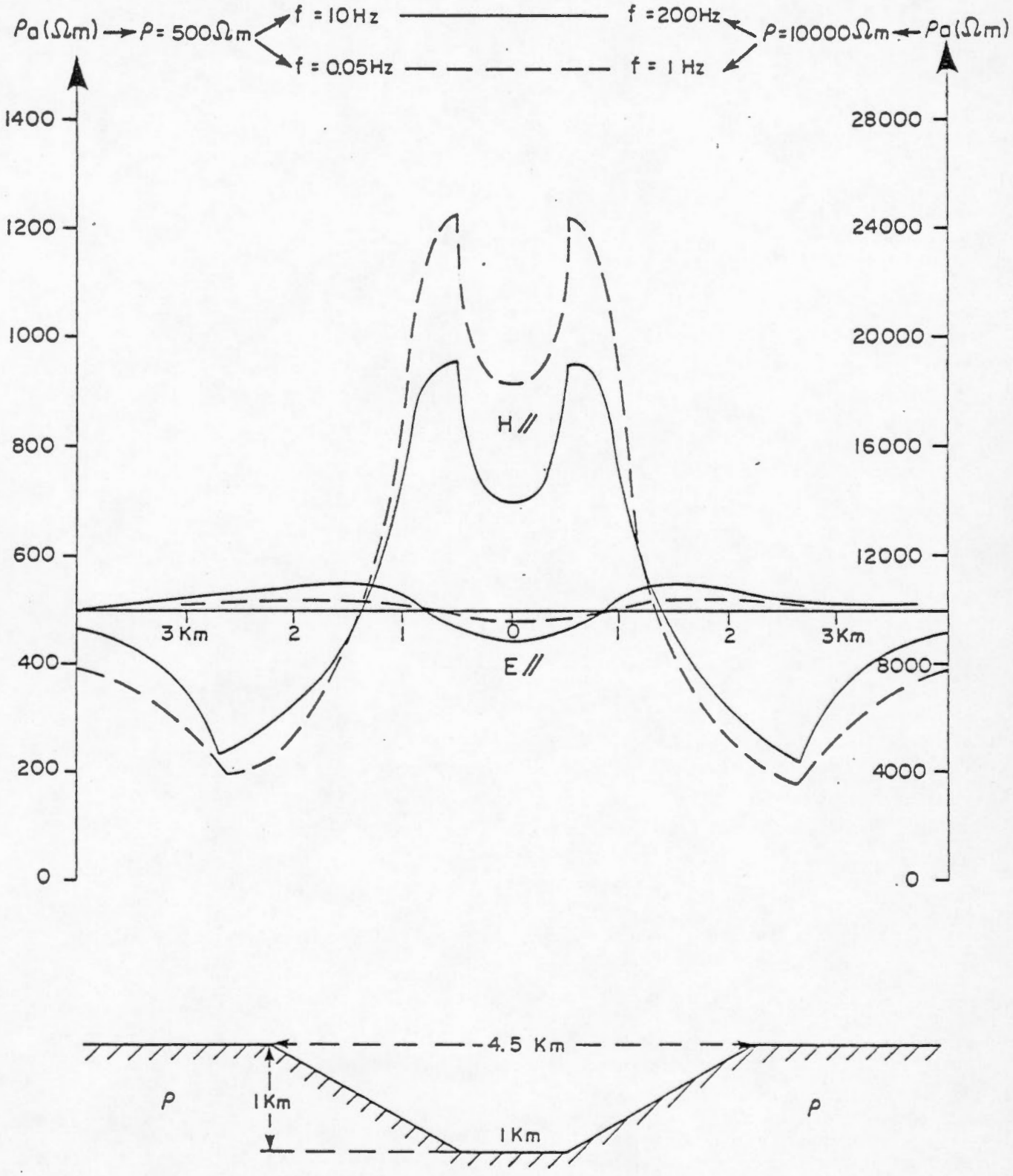

FIGURE 4. Effet topographique d'une vallée.

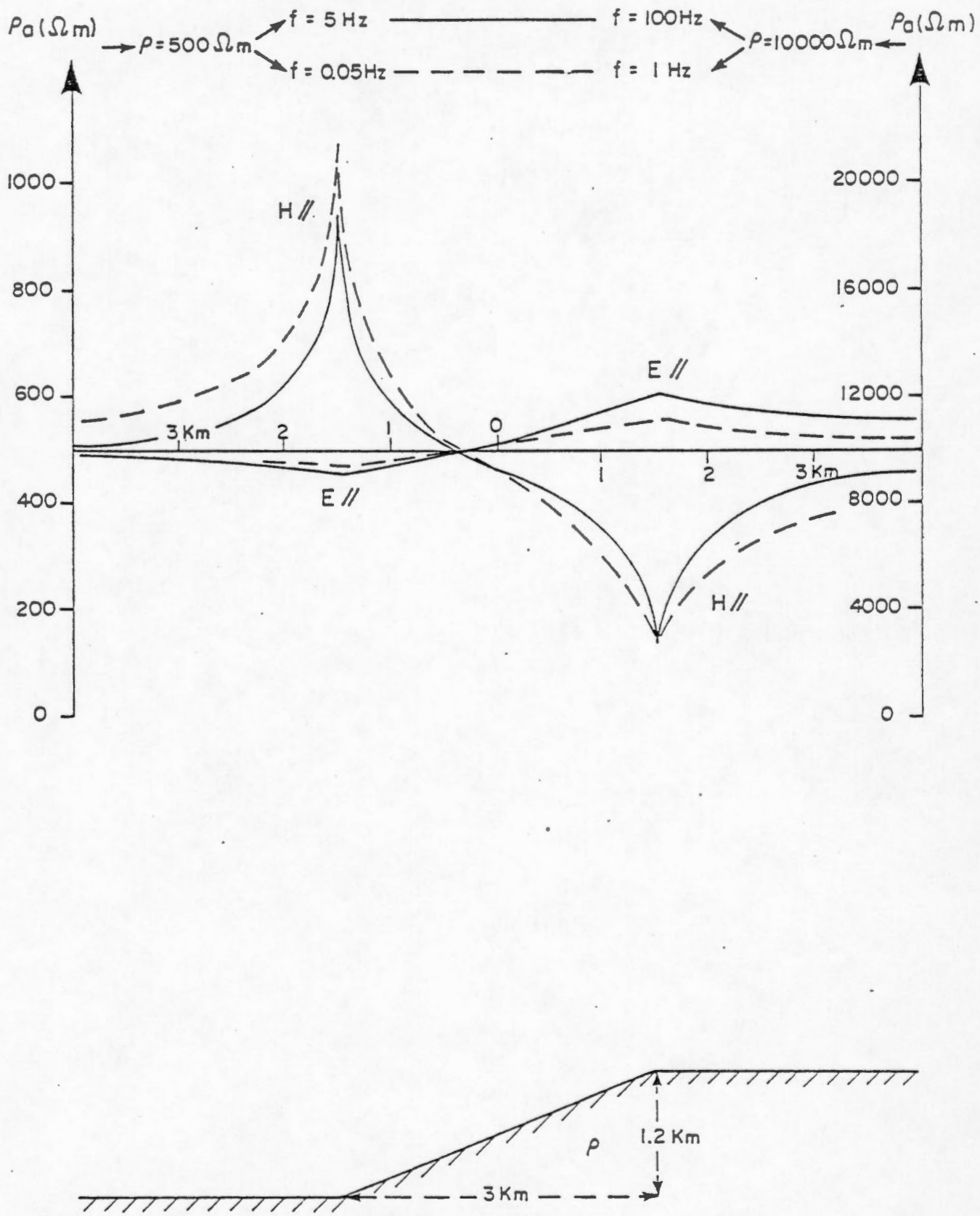

FIGURE 5. Effet topographique d'une pente.

FIGURE 6. Mount Meager - Courbes de sondage M.T. de la station ME.1.

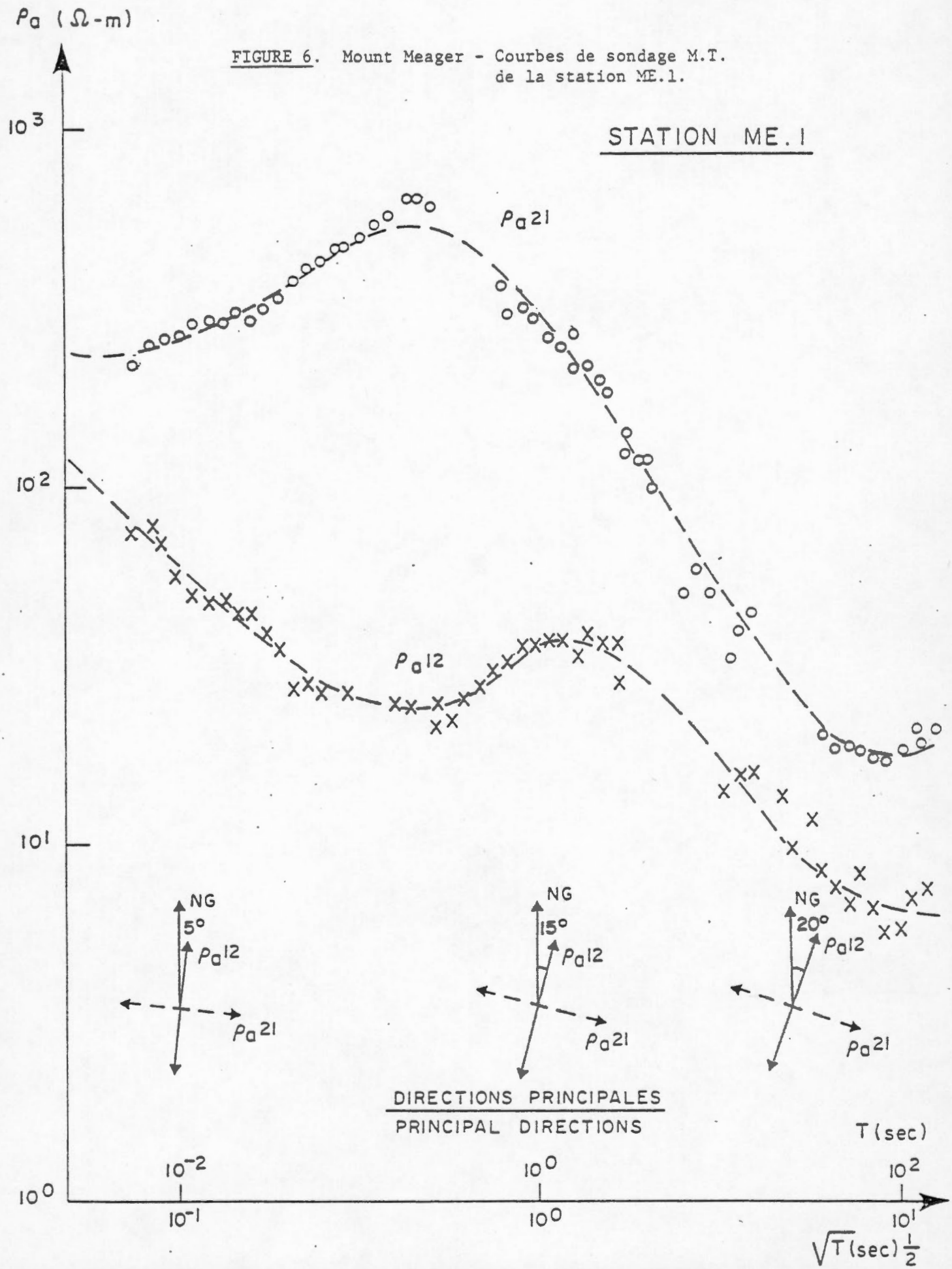

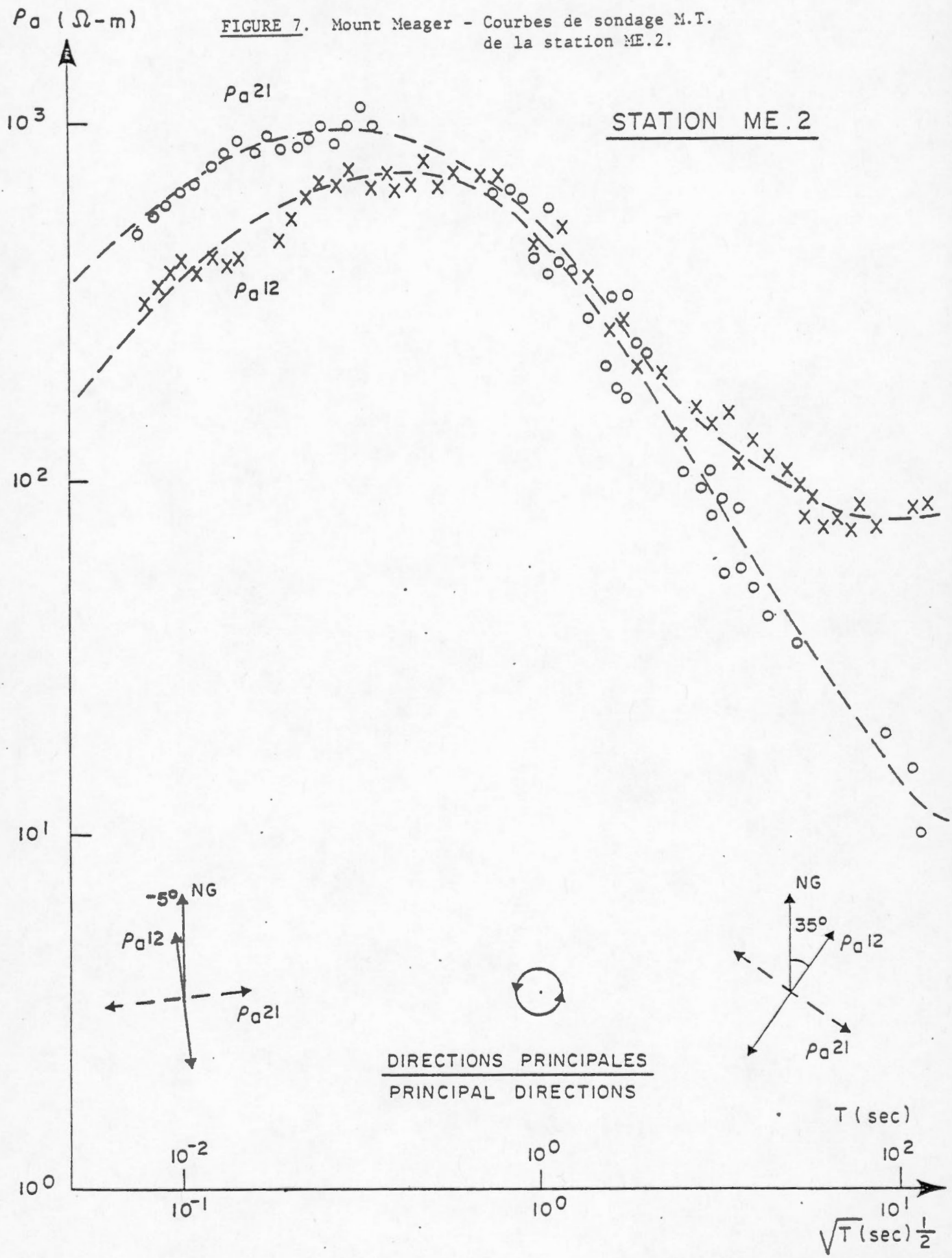

FIGURE 7. Mount Meager - Courbes de sondage M.T. de la station ME.2.

FIGURE 8. Mount Meager - Courbes de sondage M.T. de la station ME.3.

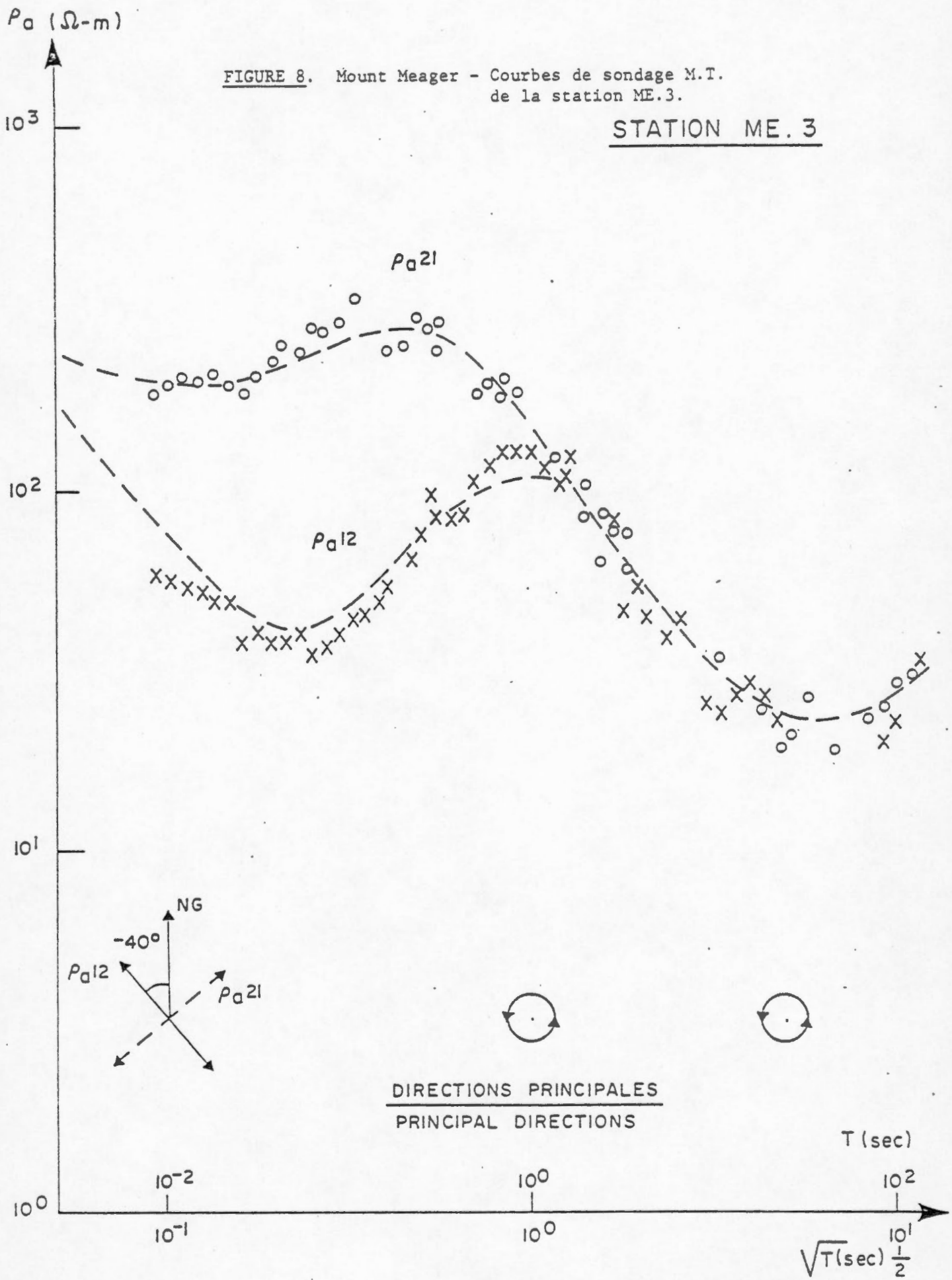

FIGURE 9. Mount Meager - Courbes de sondage M.T. de la station ME.4.

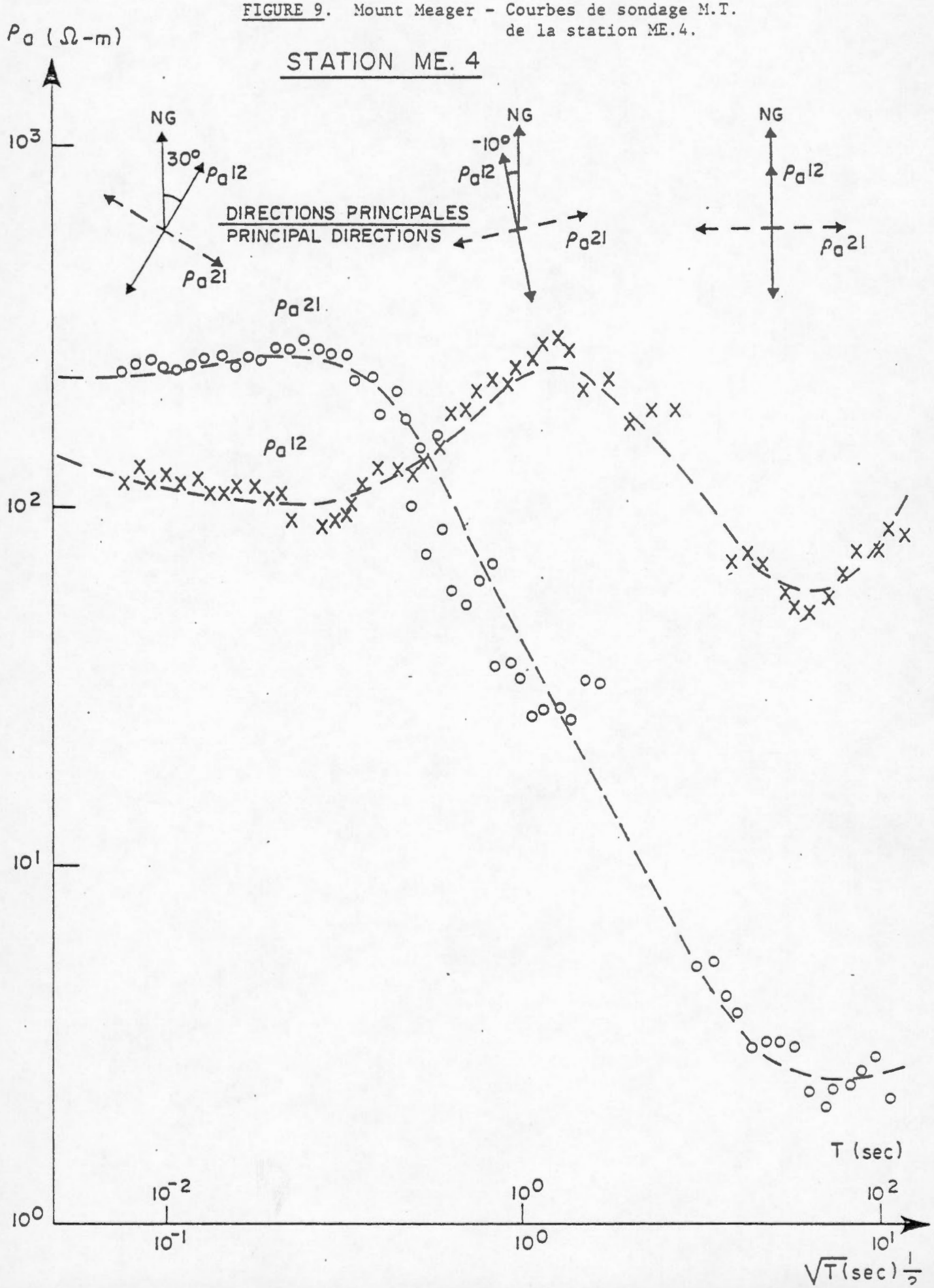

FIGURE 10. Mount Meager - Courbes de sondage suivant la direction principale N.S.

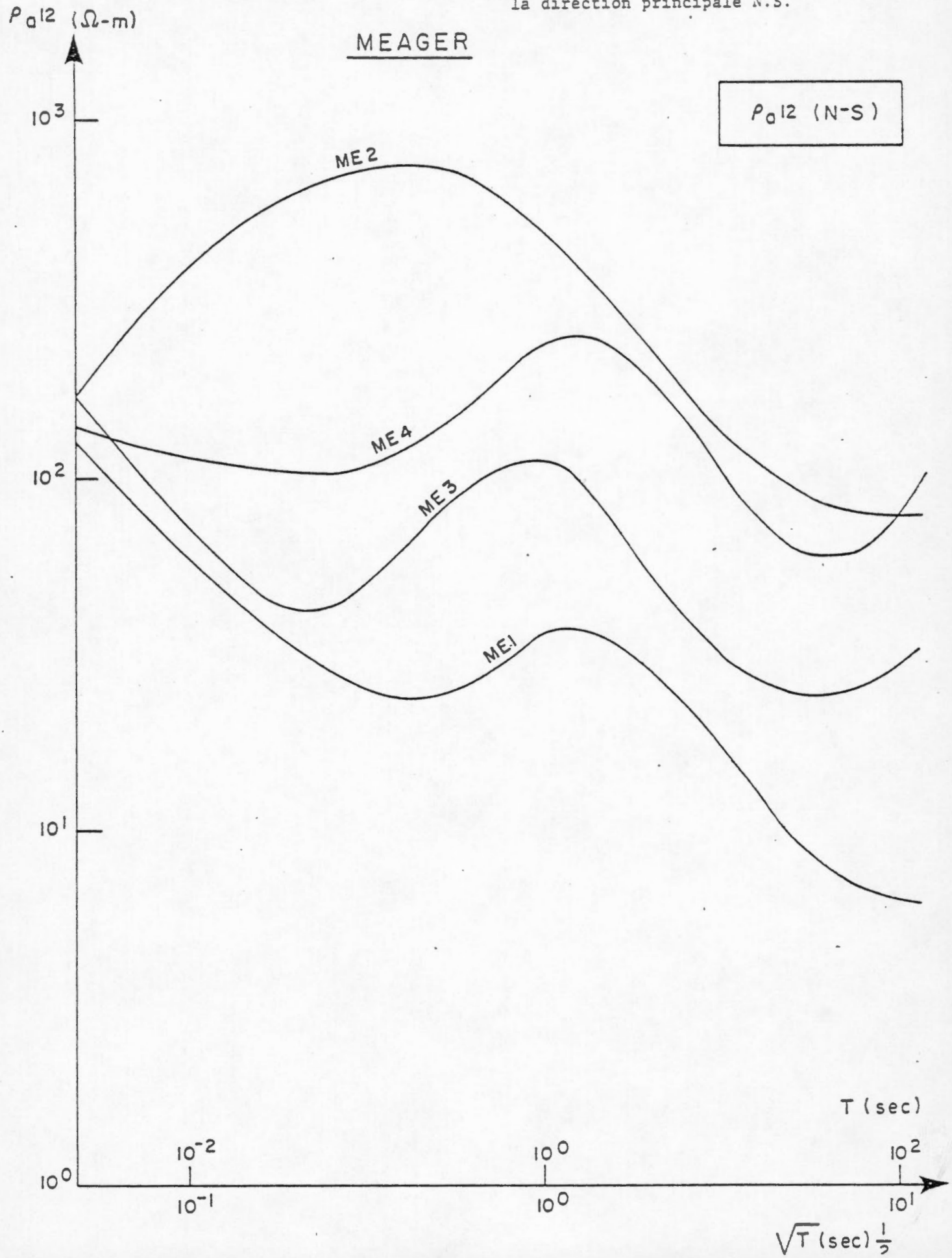

FIGURE 11. Mount Meager - Courbes de sondage suivant la direction principale E.W.

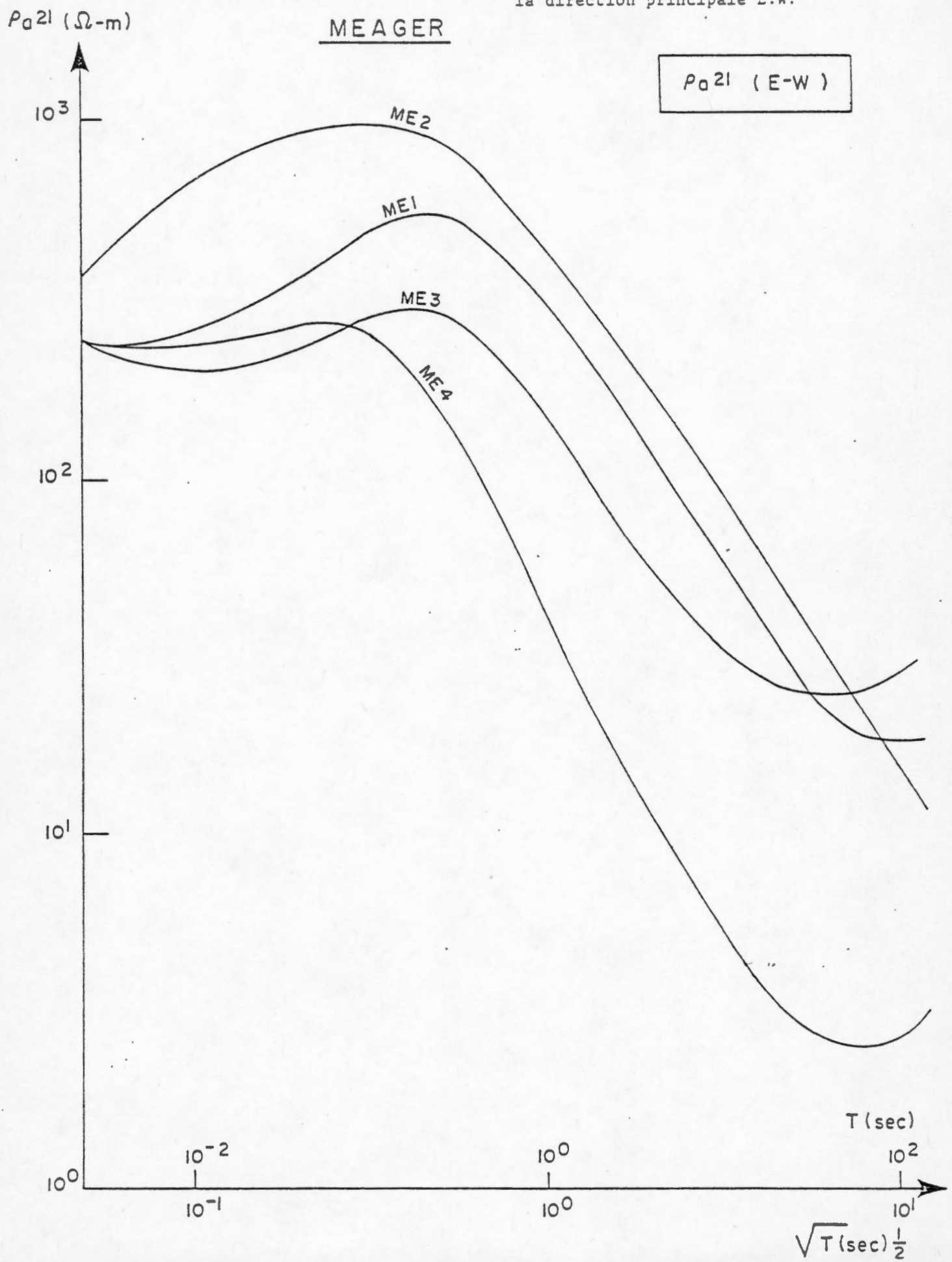

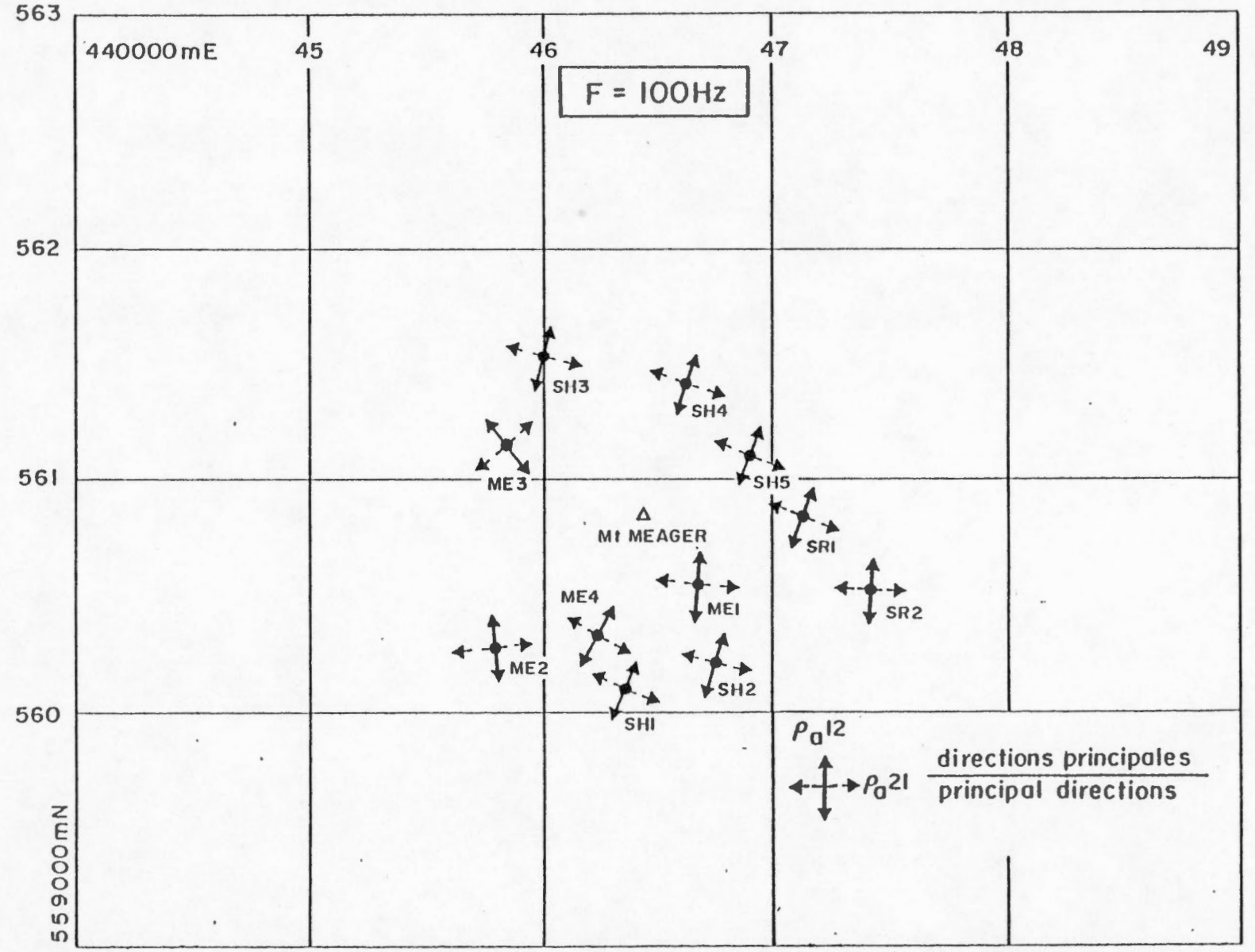

FIGURE 12. Mount Meager - Carte des directions principales, F = 100 Hz.

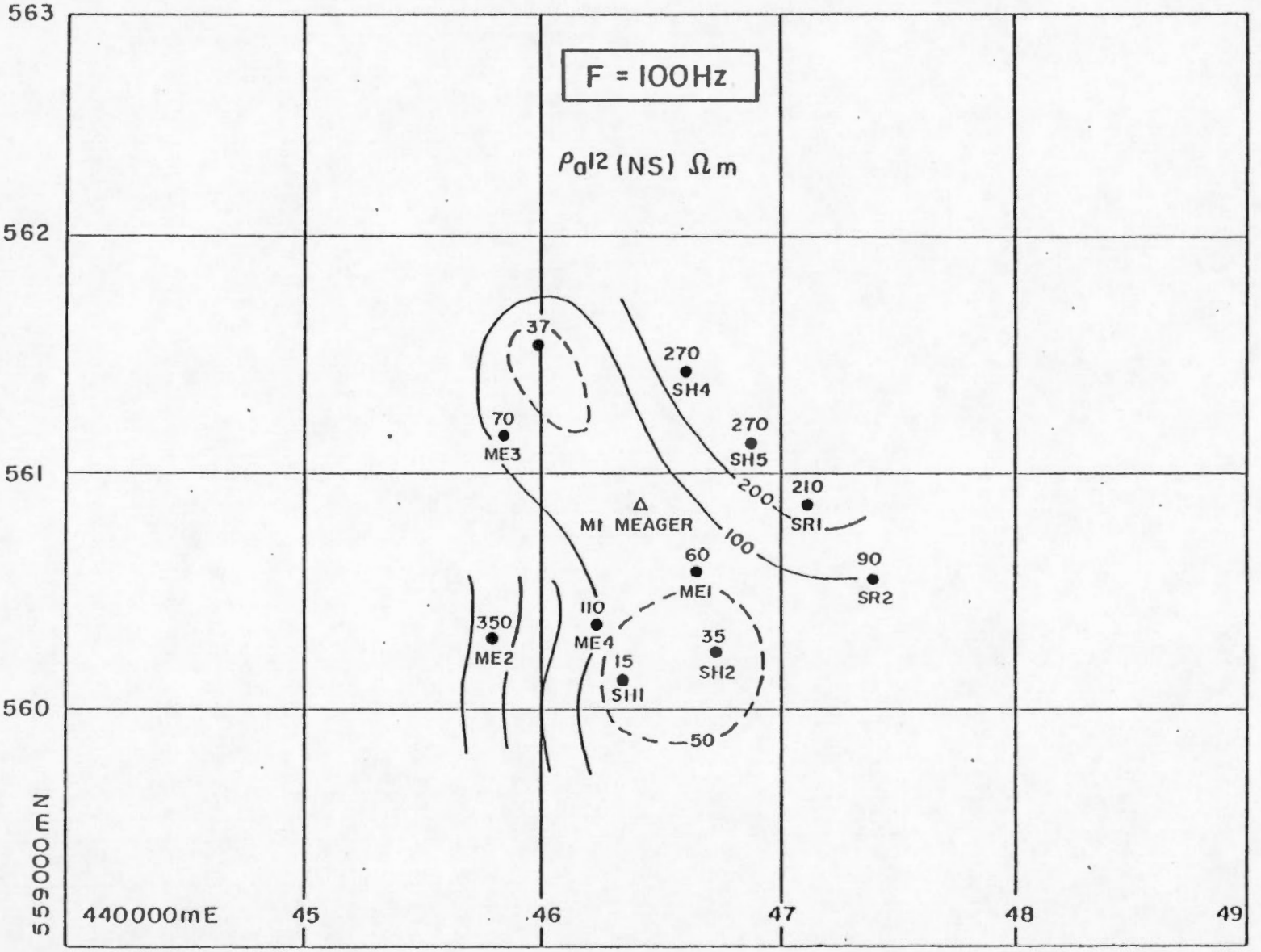

FIGURE 13. Mount Meager - Carte des résistivités apparentes ρ_{a12} (NS), F = 100 Hz.

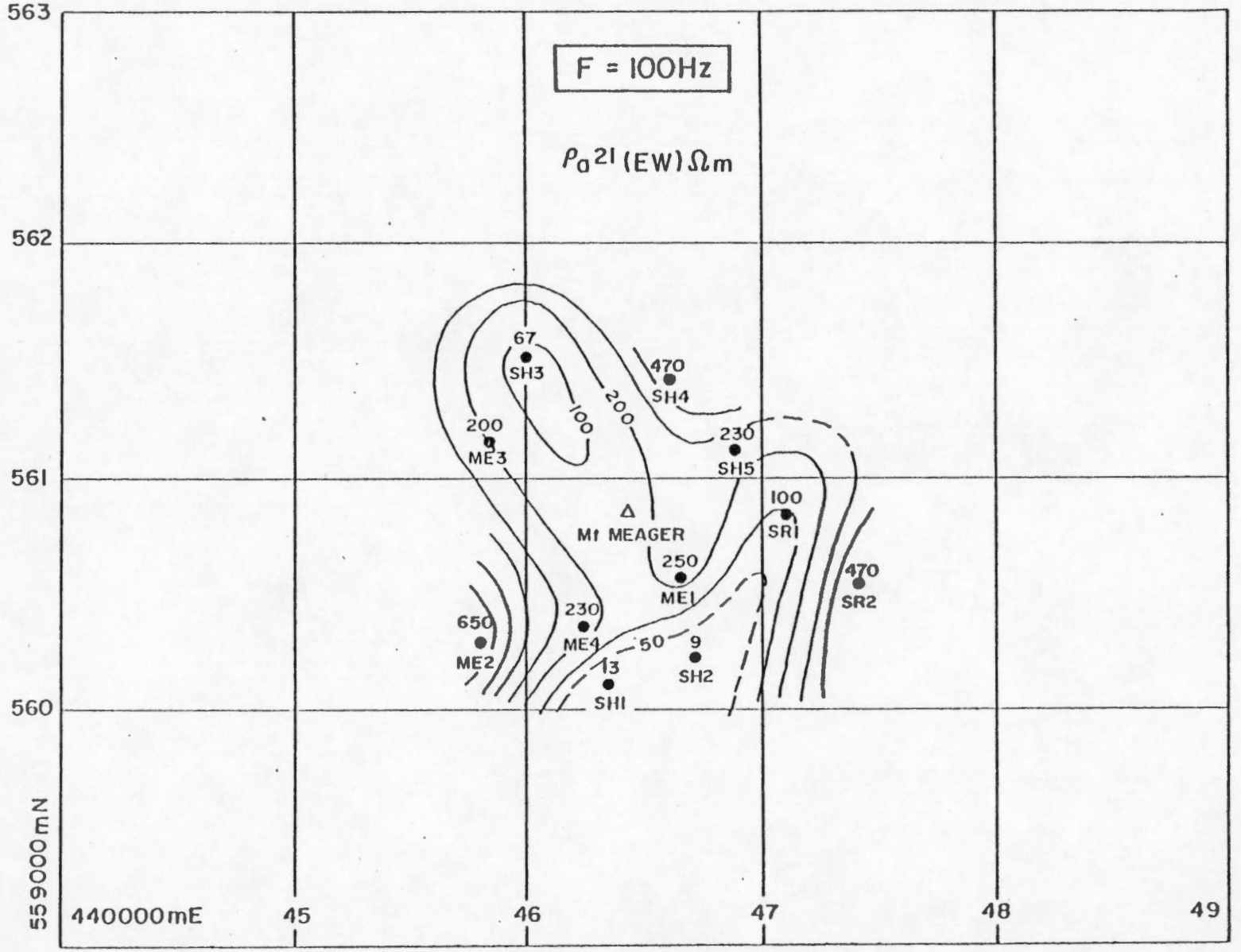

FIGURE 14. Mount Meager - Carte des résistivités apparentes ρ_{a21} (EW), F = 100 Hz.

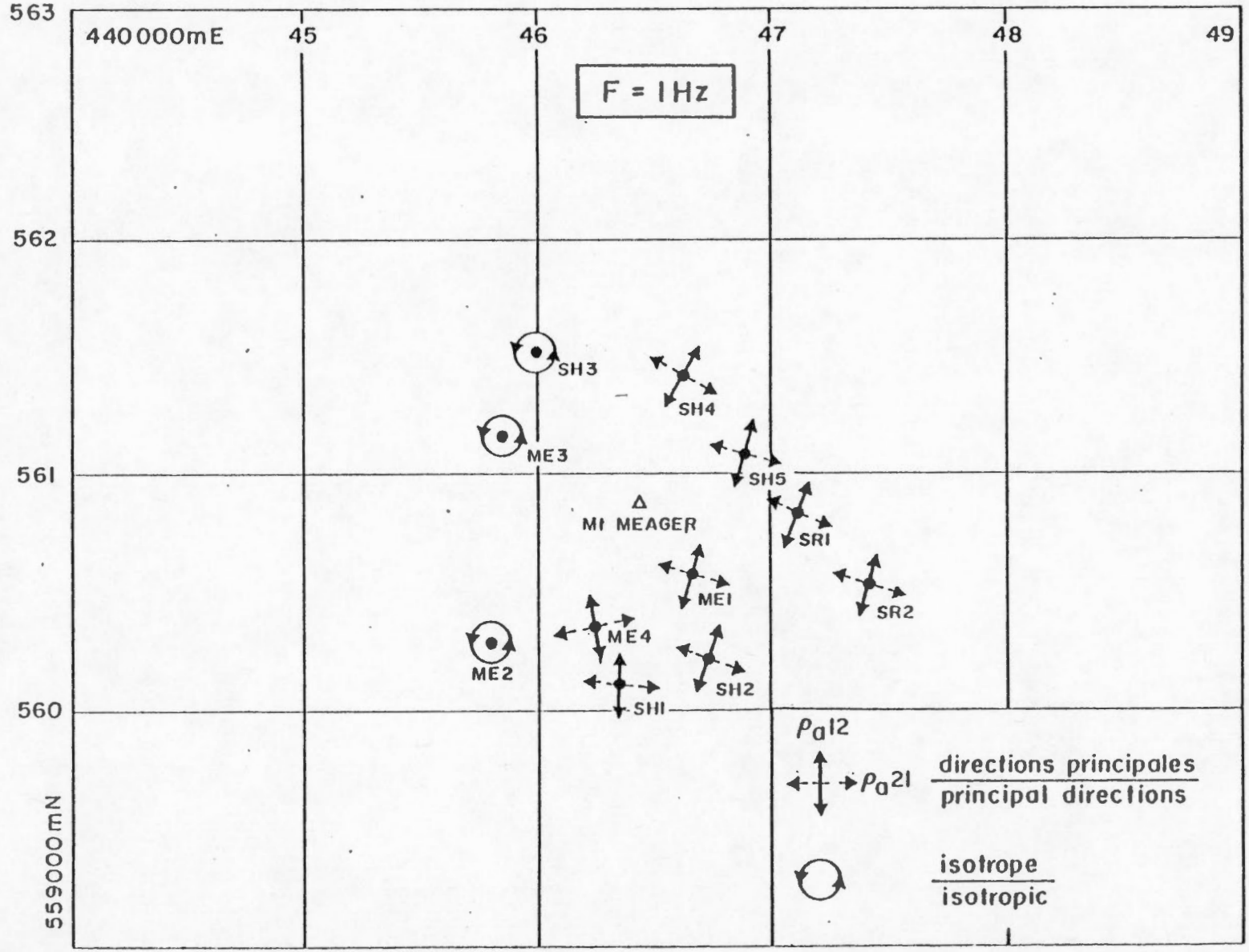

FIGURE 15. Mount Meager - Carte des directions principales, F = 1 Hz.

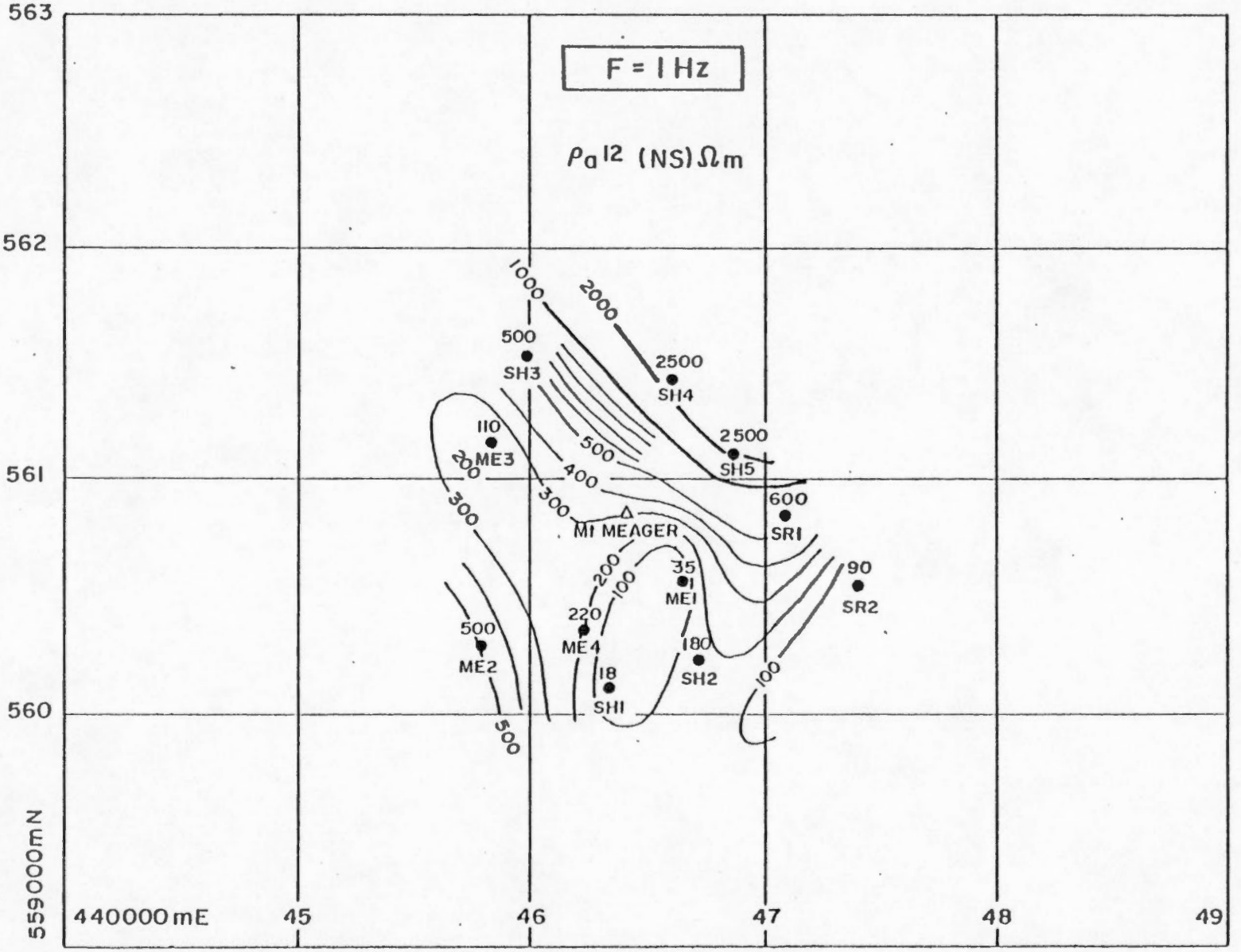

FIGURE 16. Mount Meager - Carte des résistivités apparentes ρ_{a12} (NS), F = 1 Hz.

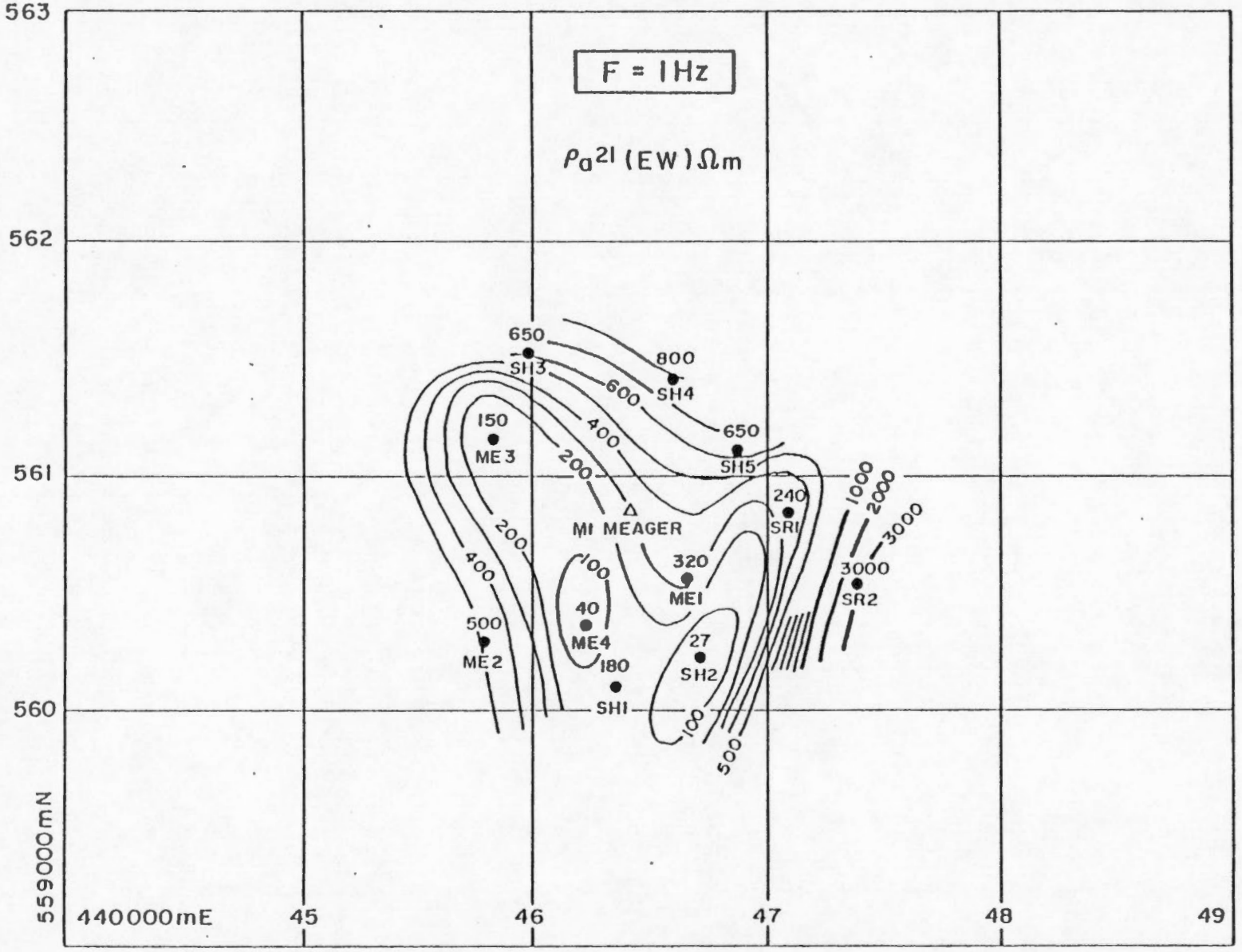

FIGURE 17. - Mount Meager - Carte des résistivités apparentes ρ_{a21} (EW), F = 1 Hz.

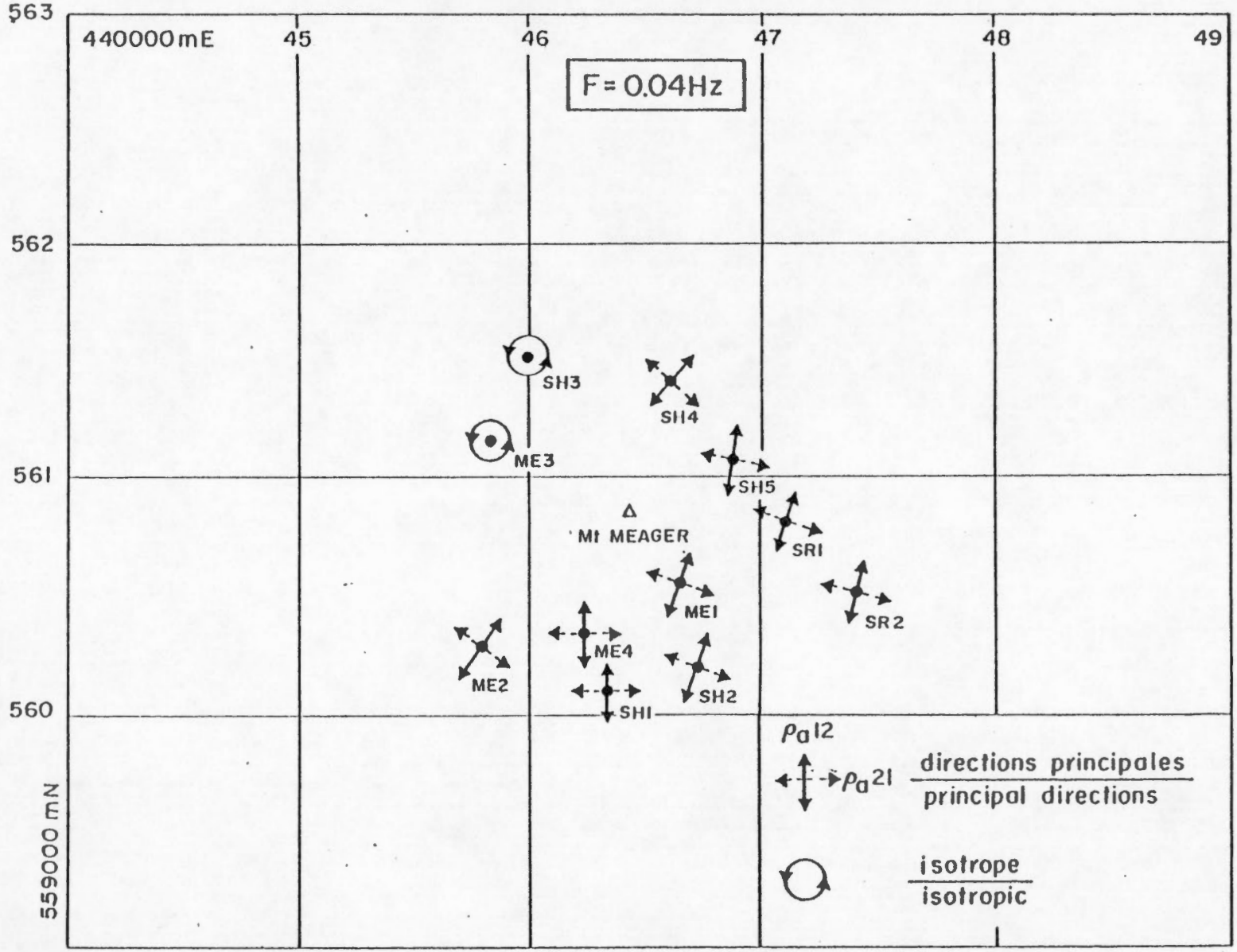

FIGURE 18. Mount Meager - Carte des directions principales, F = 0.04 Hz.

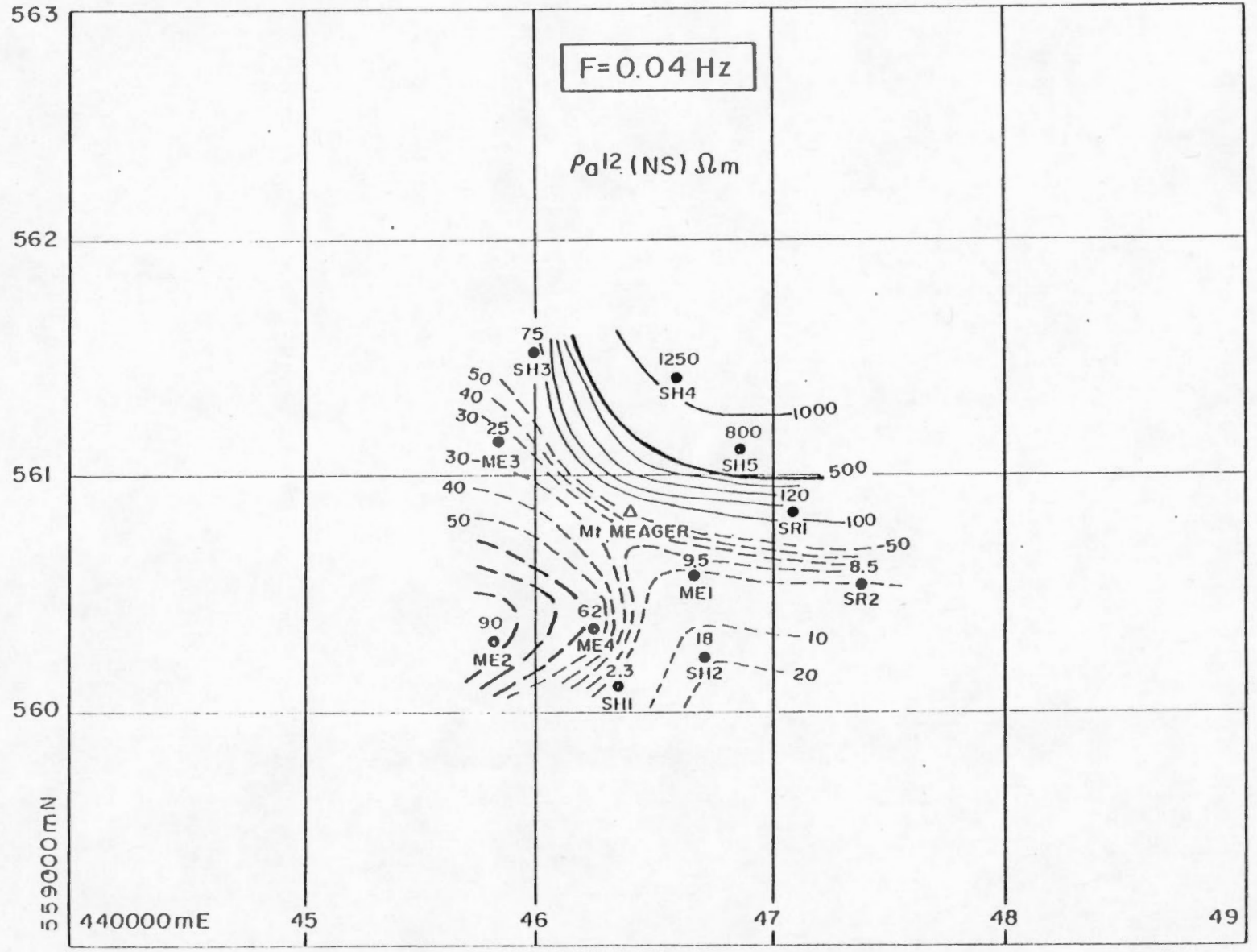

FIGURE 19. Mount Meager - Carte des résistivités apparentes ρ_{a12}(NS), F = 0.04 Hz.

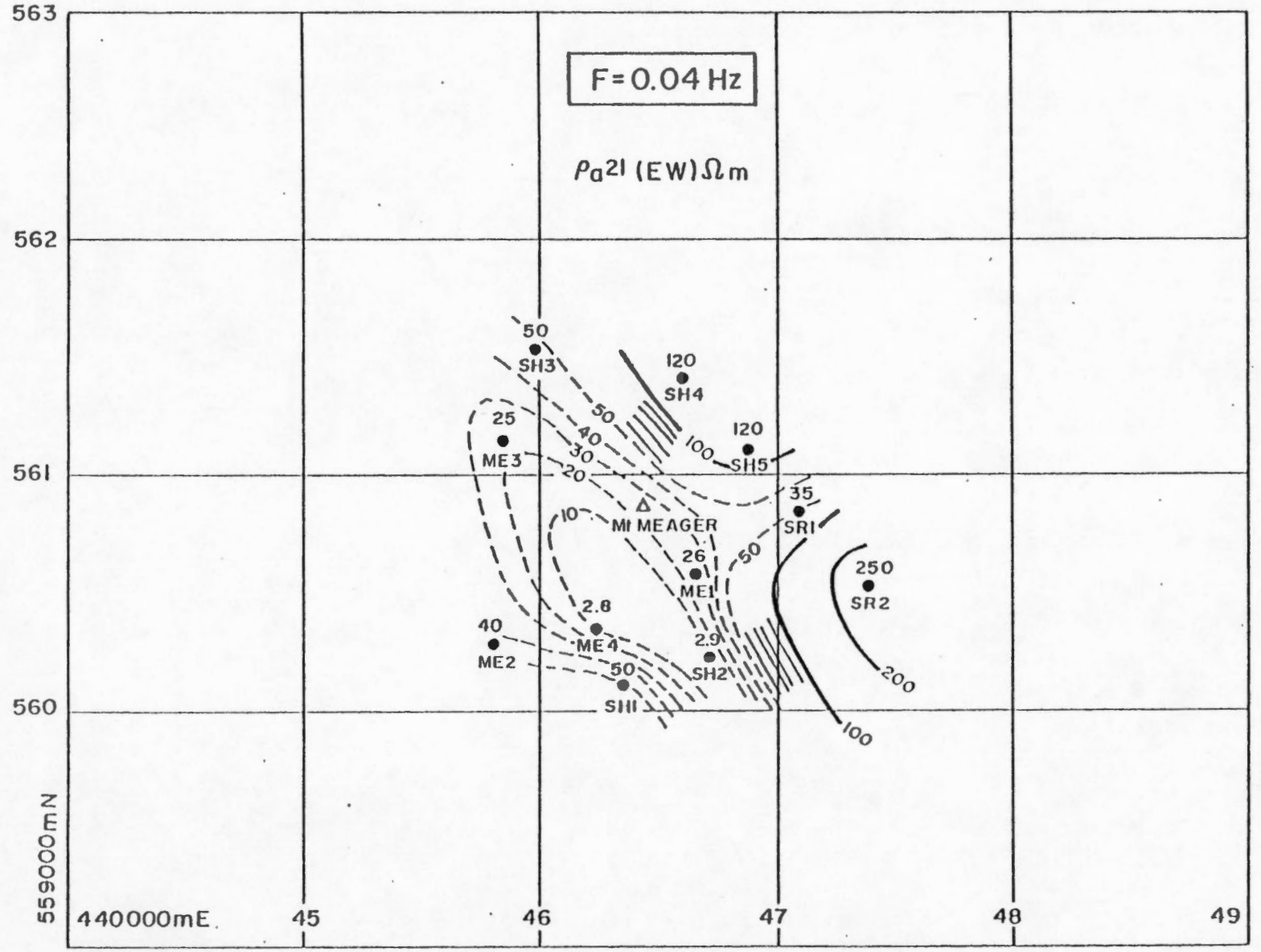

FIGURE 20. Mount Meager - Carte des résistivités apparentes ρ_{a21} (EW), F = 0.04 Hz.

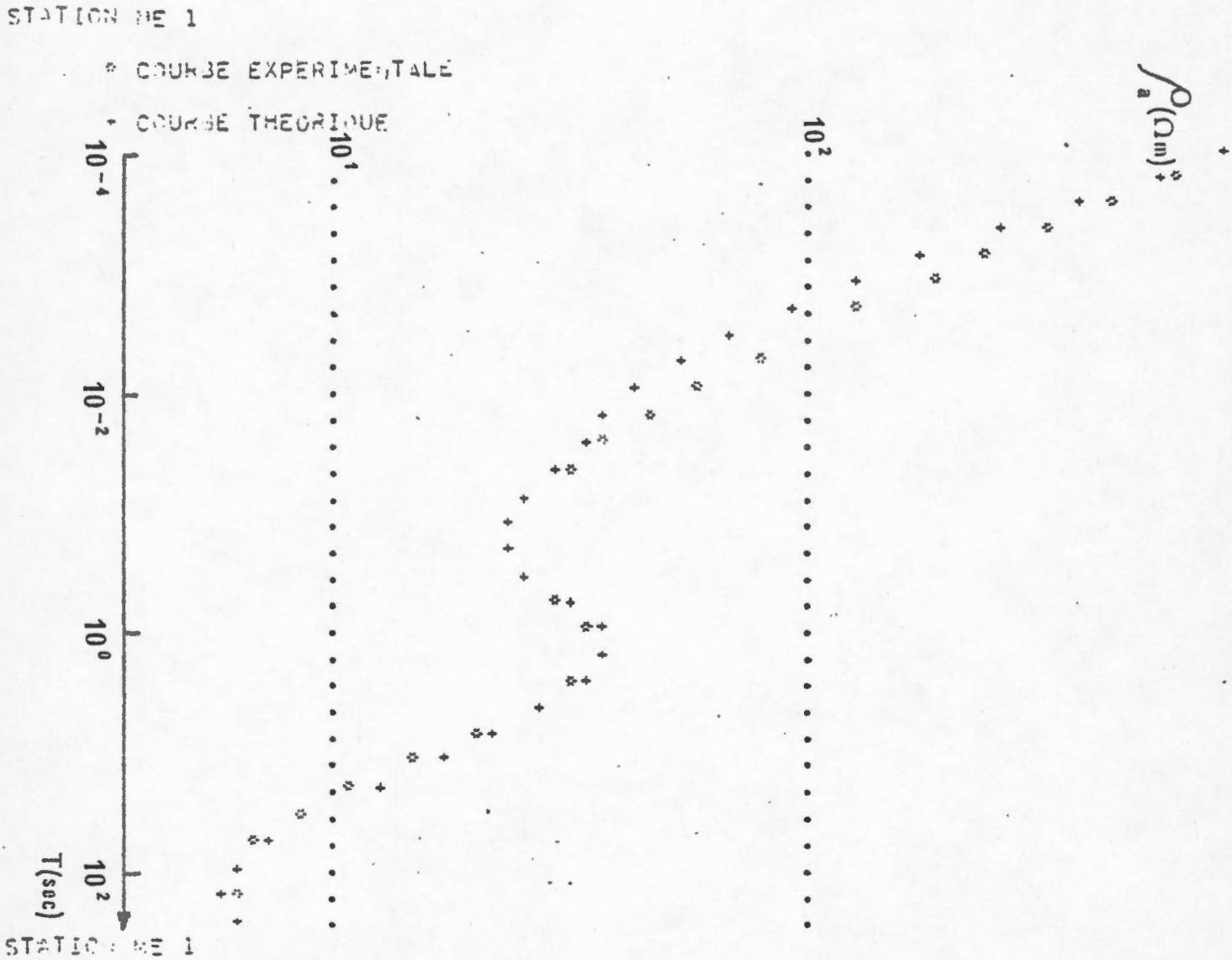

STATION ME 1

ρ 1= .300000E+03Ωm H 1= .100000E+00km

ρ 2= .200000E+02 H 2= .100000E+01

ρ 3= .970000E+02 H 3= .250000E+01

ρ 4= .220000E+01 H 4= .100000E+02

ρ 5= .140000E+03 H 5= ∞

FIGURE 21. Mount Meager - Interprétation de la courbe $\rho_{a_{12}}$(NS) de la station ME.1.

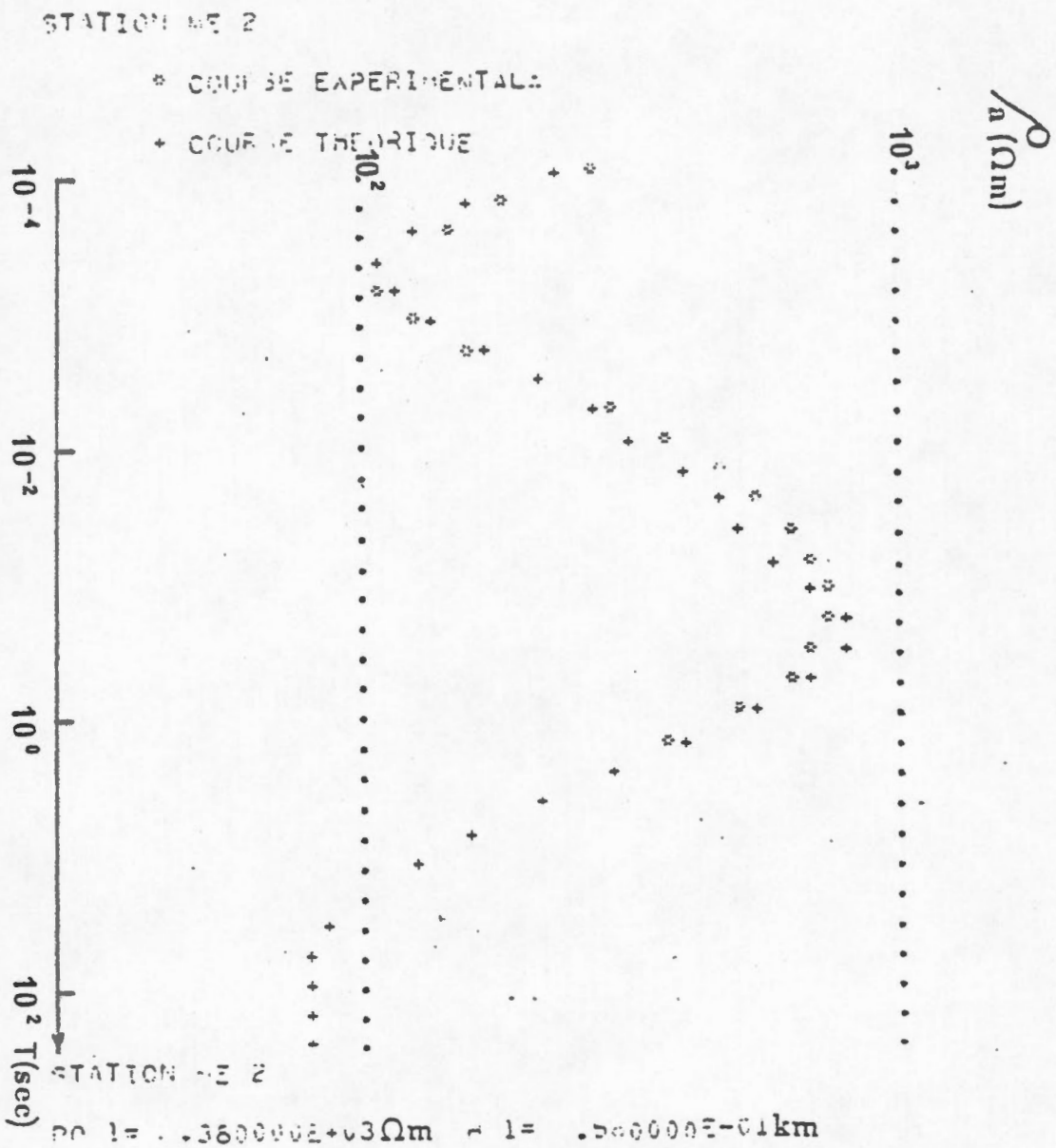

STATION ME 2

RO 1= .3600000E+03Ωm H 1= .5000000E-01km

RO 2= .6000000E+01 H 2= .5000000E-02

RO 3= .1000000E+03 H 3= .8000000E+01

RO 4= .4000000E+02 H 4= .1200000E+02

RO 5= .1000000E+03 H 5= ∞

FIGURE 22. Mount Meager - Interprétation de la courbe $\rho_{a_{12}}$(NS) de la station ME.2.

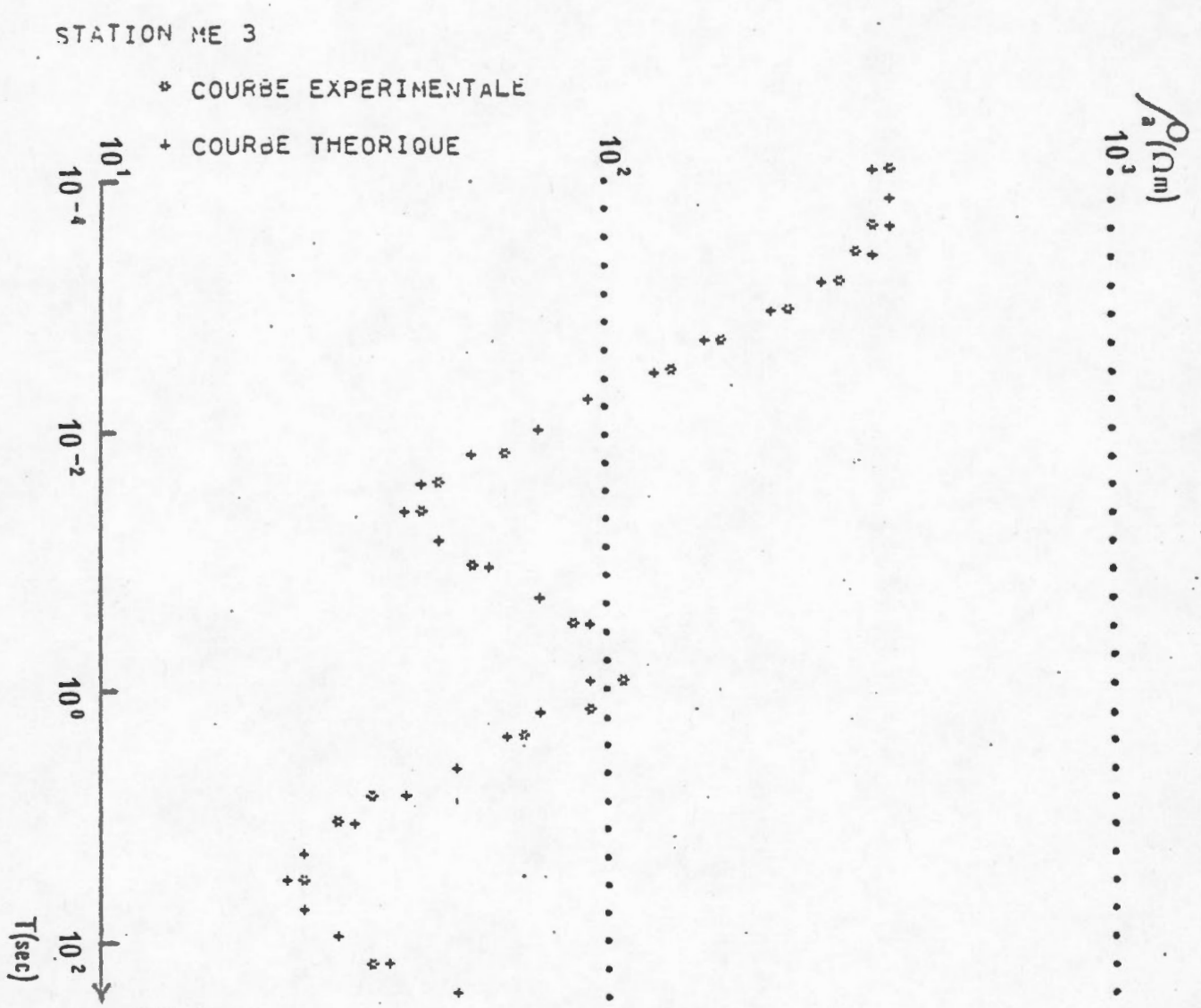

STATION ME 3

RO 1=	.315000E+03 Ωm	H 1=	.165000E+00 km
RO 2=	.260000E+02	H 2=	.430000E+00
RO 3=	.350000E+03	H 3=	.280000E+01
RO 4=	.160000E+02	H 4=	.100000E+02
RO 5=	.300000E+03	H 5=	∞

FIGURE 23. Mount Meager - Interprétation de la courbe $\rho_{a_{12}}$(NS) de la station ME.3.

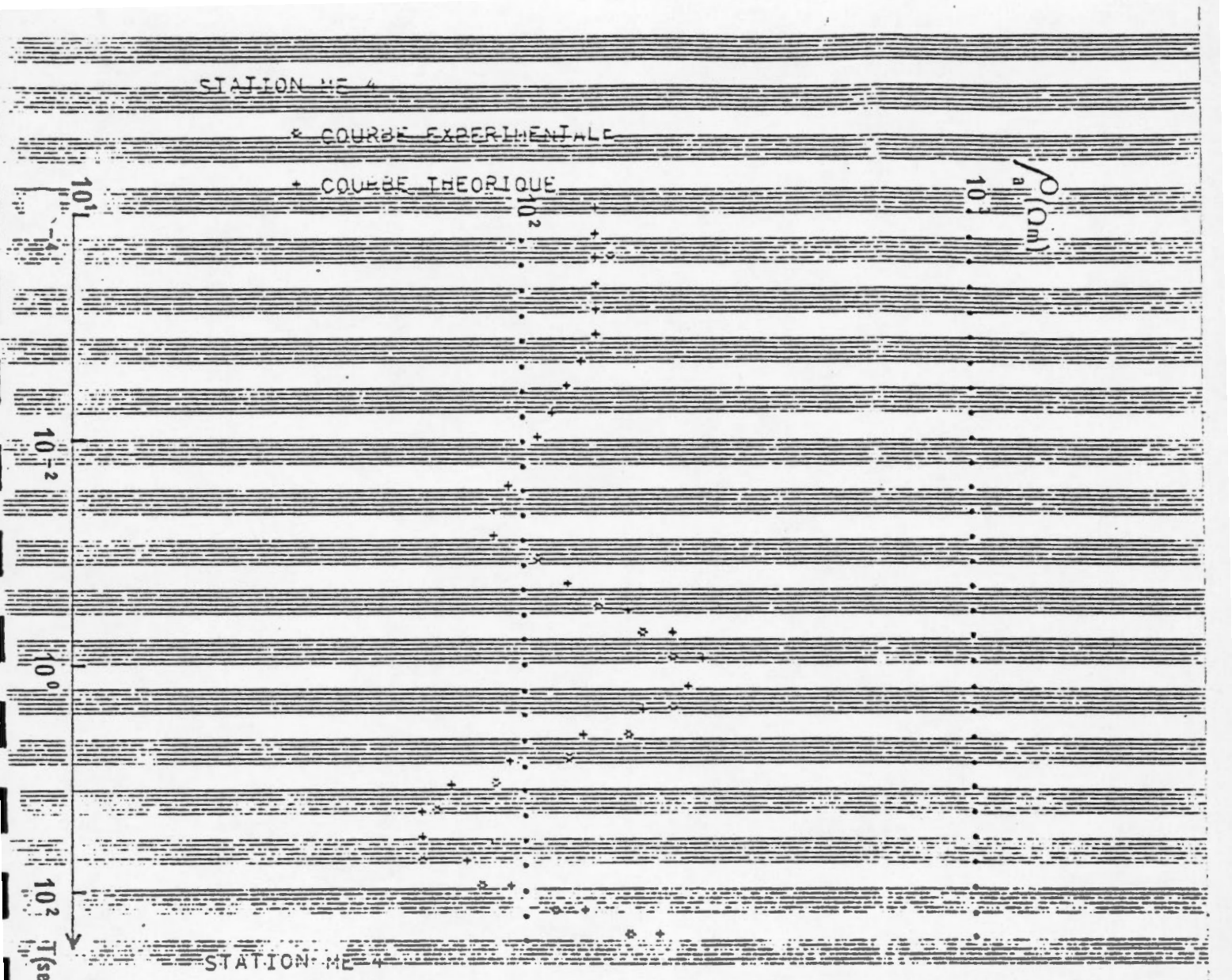

STATION ME 4

RO 1= .150000E+03Ωm H 1= .165000E+00km

RO 2= .850000E+02 H 2= .100000E+01

RO 3= .550000E+03 H 3= .700000E+01

RO 4= .180000E+02 H 4= .550000E+01

RO 5= .200000E+04 H 5= ∞

FIGURE 24. Mount Meager - Interprétation de la courbe $D_{a_{12}}$ (NS) de la station ME 4

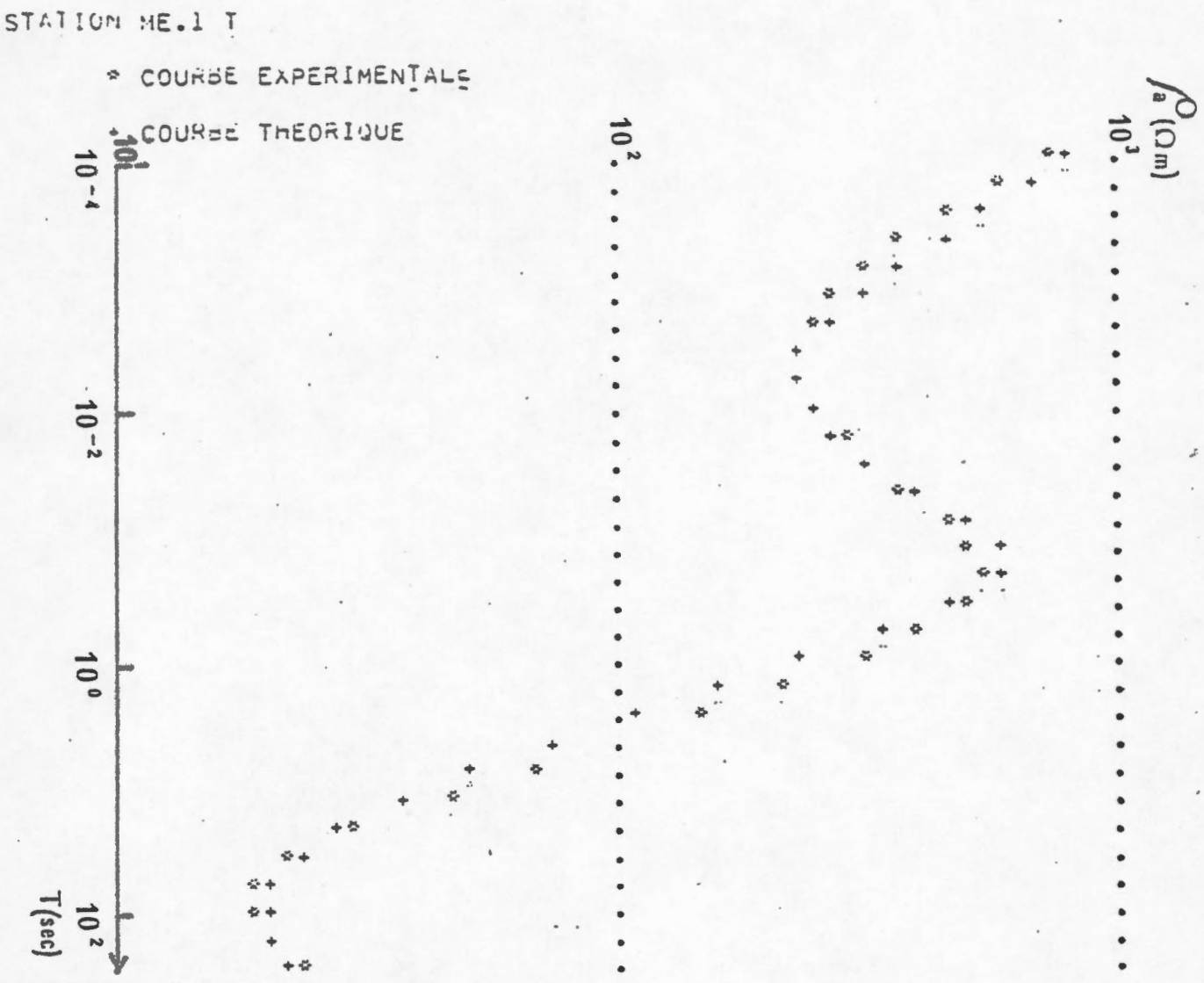

STATION ME.1 T

RO 1=	.950000E+03Ωm	H 1=	.100000E-00km
RO 2=	.130000E+03	H 2=	.400000E+00
RO 3=	.740000E+03	H 3=	.450000E+01
RO 4=	.800000E+01	H 4=	.500000E+01
RO 5=	.300000E+02	H 5=	∞

FIGURE 25. Mount Meager - Interprétation de la courbe $\rho_{a_{21}}$ (EW) de la station ME.1.

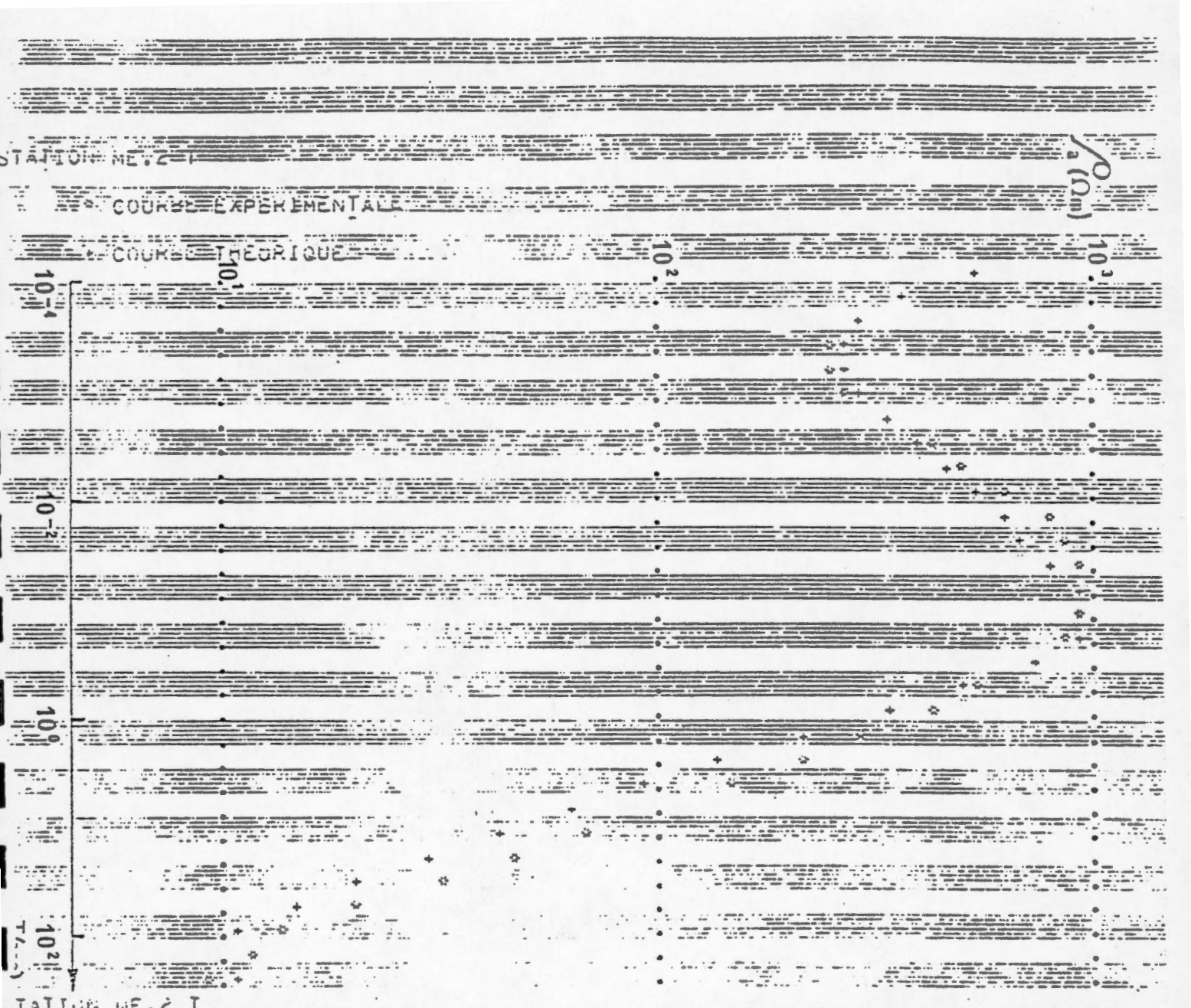

FIGURE 26. Mount Meager - Interprétation de la courbe $\rho_{a_{21}}$ (EW) de la station ME.2.

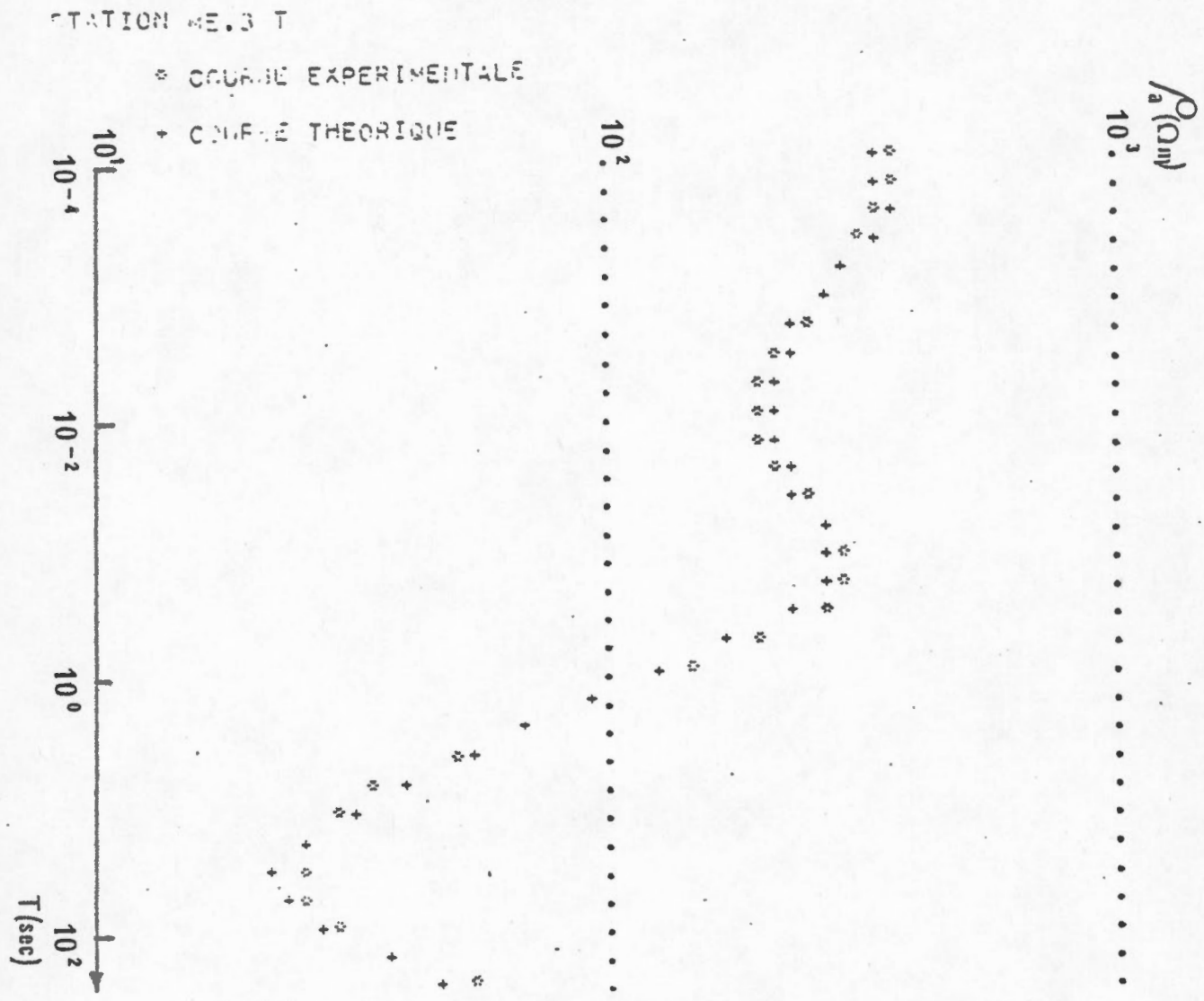

STATION ME.3 T

ρ 1=	.3[illegible]E+03 Ωm	h 1=	.200000E+00 km
ρ 2=	.[illegible]E+02	h 2=	.400000E-01
ρ 3=	.2[illegible]E+03	h 3=	.315000E+01
ρ 4=	.1[illegible]E+02	h 4=	.100000E+02
ρ 5=	.3[illegible]E+03	h 5=	∞

FIGURE 27. Mount Meager - Interprétation de la courbe $\rho_{a_{21}}$(EW) de la station ME.3.

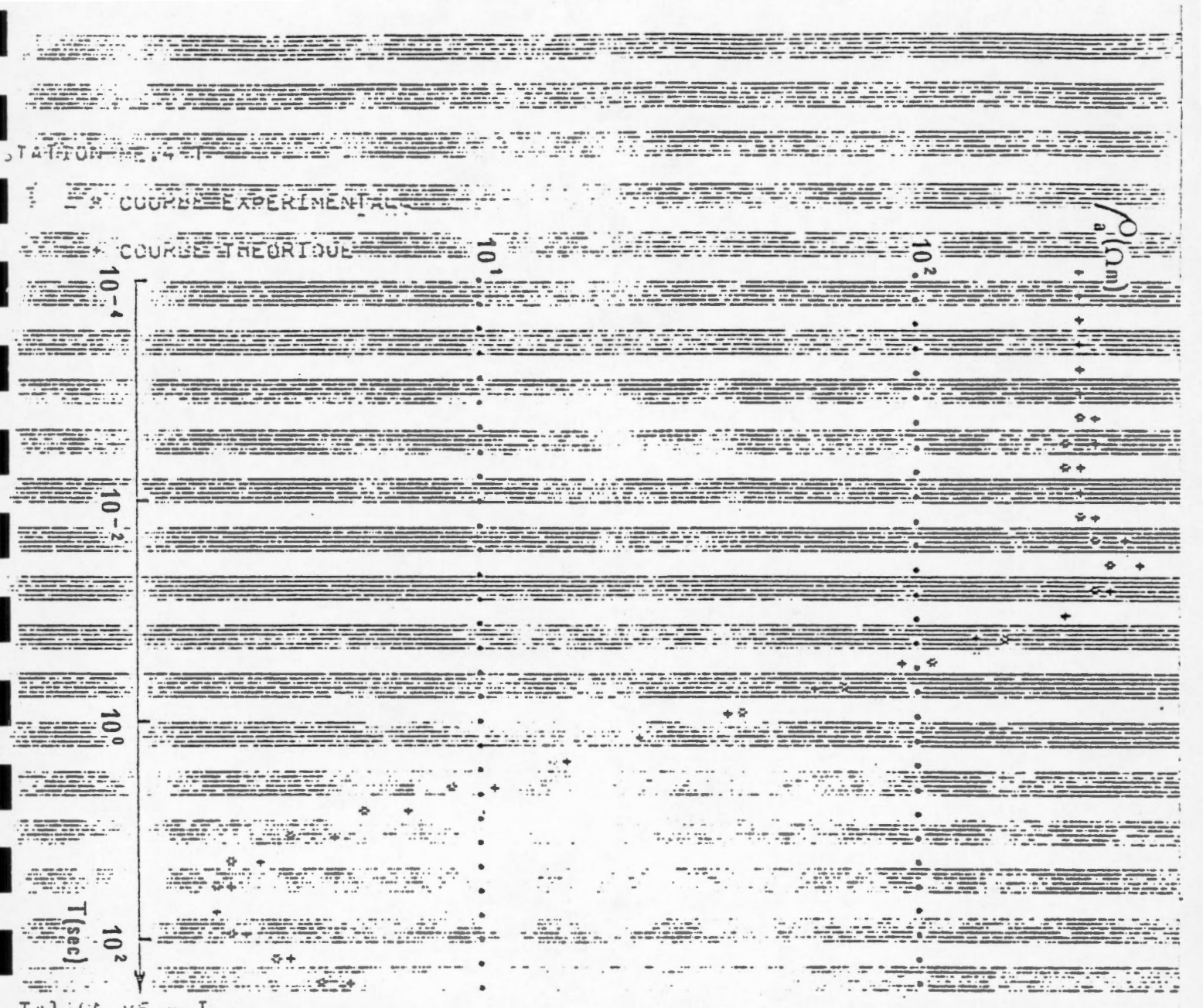

FIGURE 28. Mount Meager - Interprétation de la courbe $\rho_{a_{21}}$ (EW) de la station ME-1.

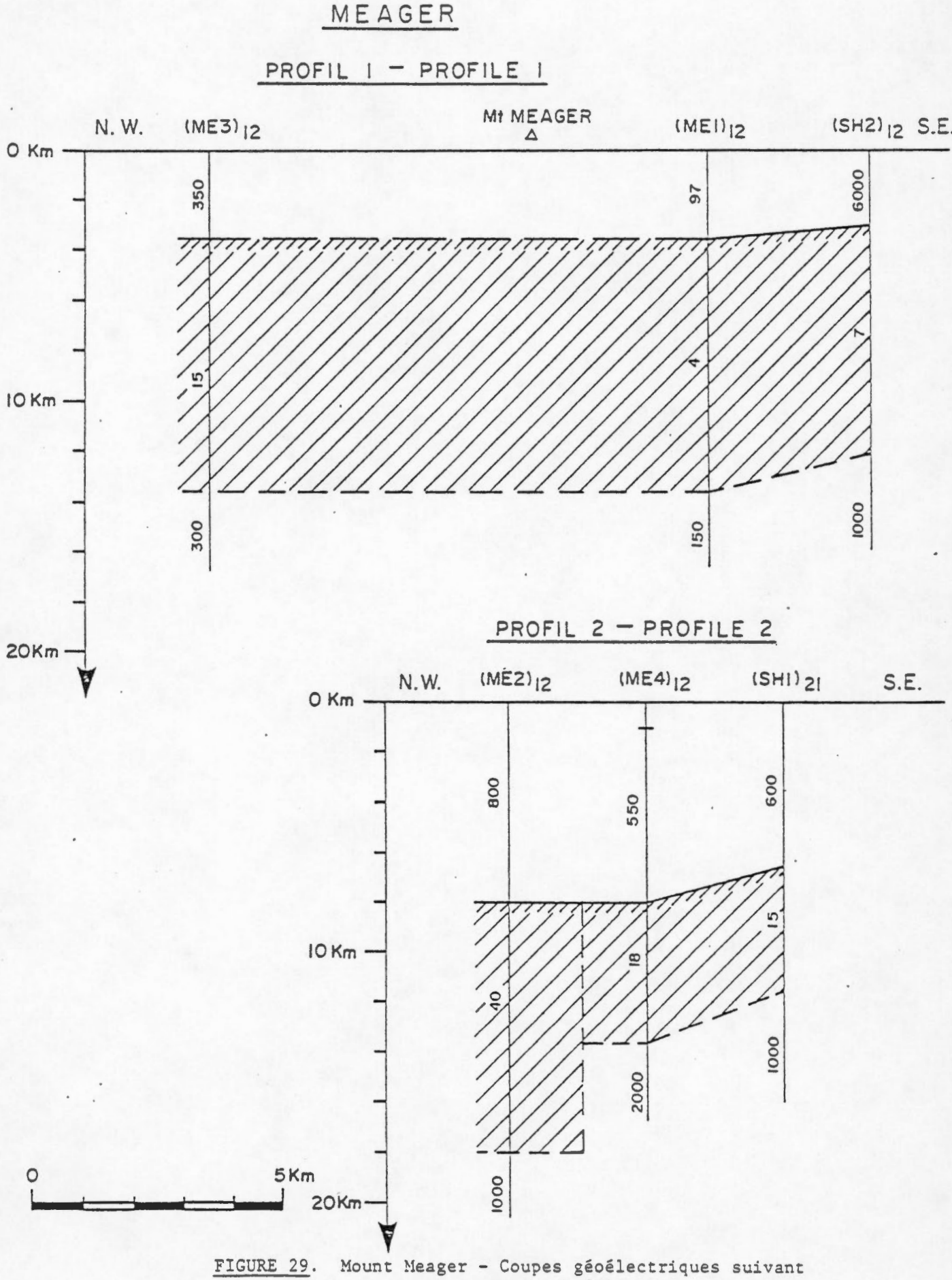

FIGURE 29. Mount Meager - Coupes géoélectriques suivant deux profils.

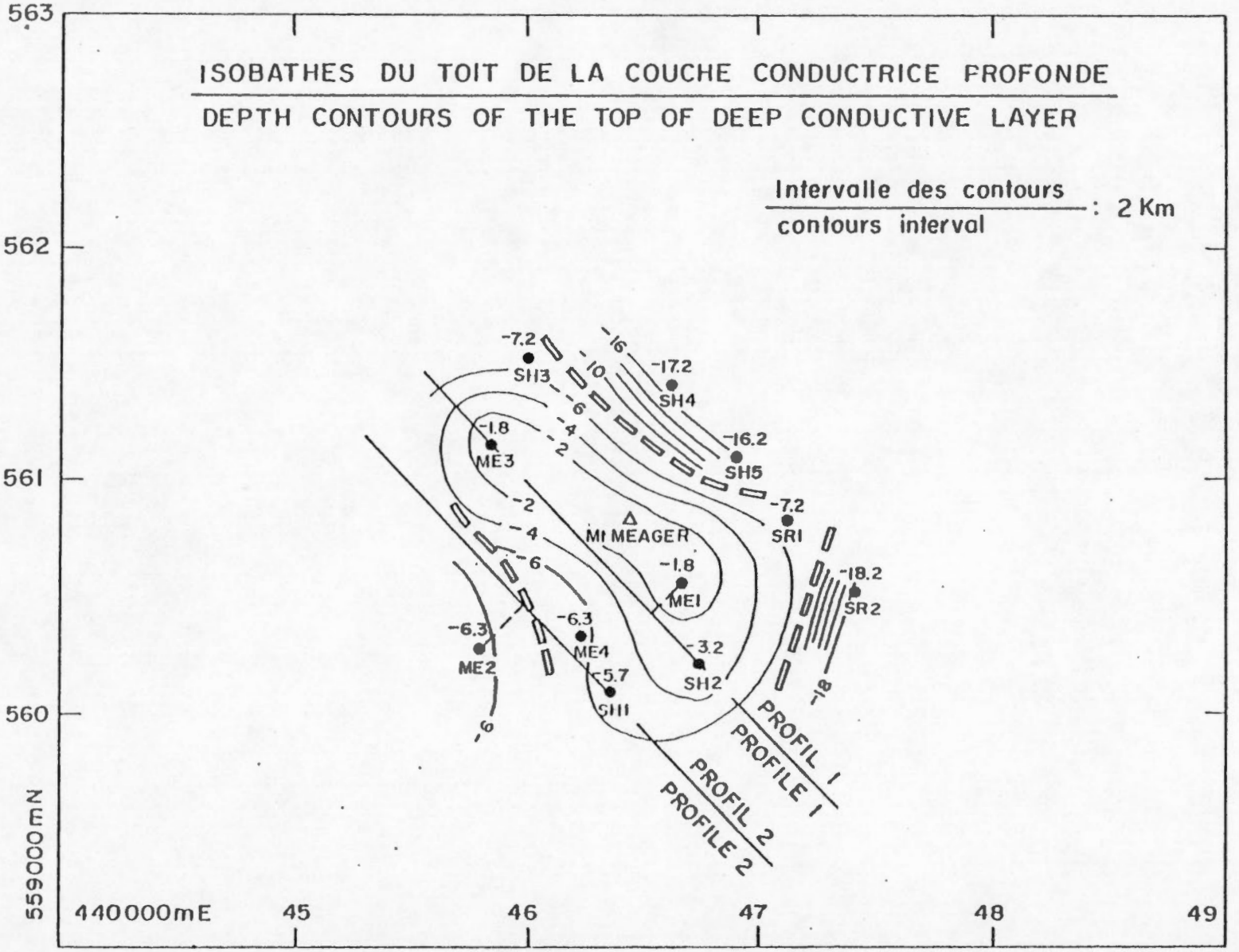

FIGURE 30. Mount Meager - Carte d'isobathes du toit de la couche conductrice profonde.

FIGURE 31. Vallée de Squamish - Courbes de sondage M.T. de la station SQ.1.

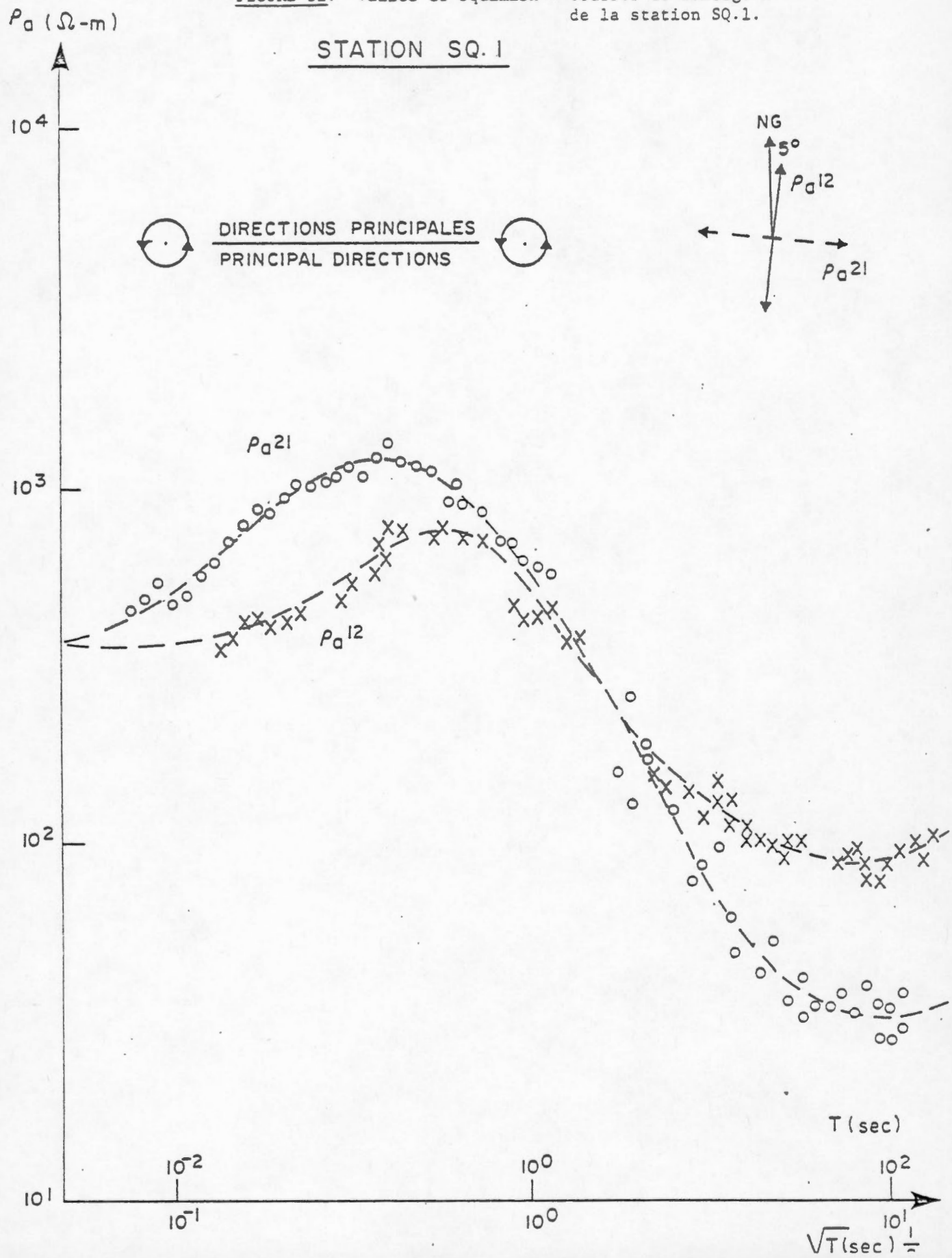

FIGURE 32. Vallée de Squamish - Courbes de sondage M.T. de la station SQ.2.

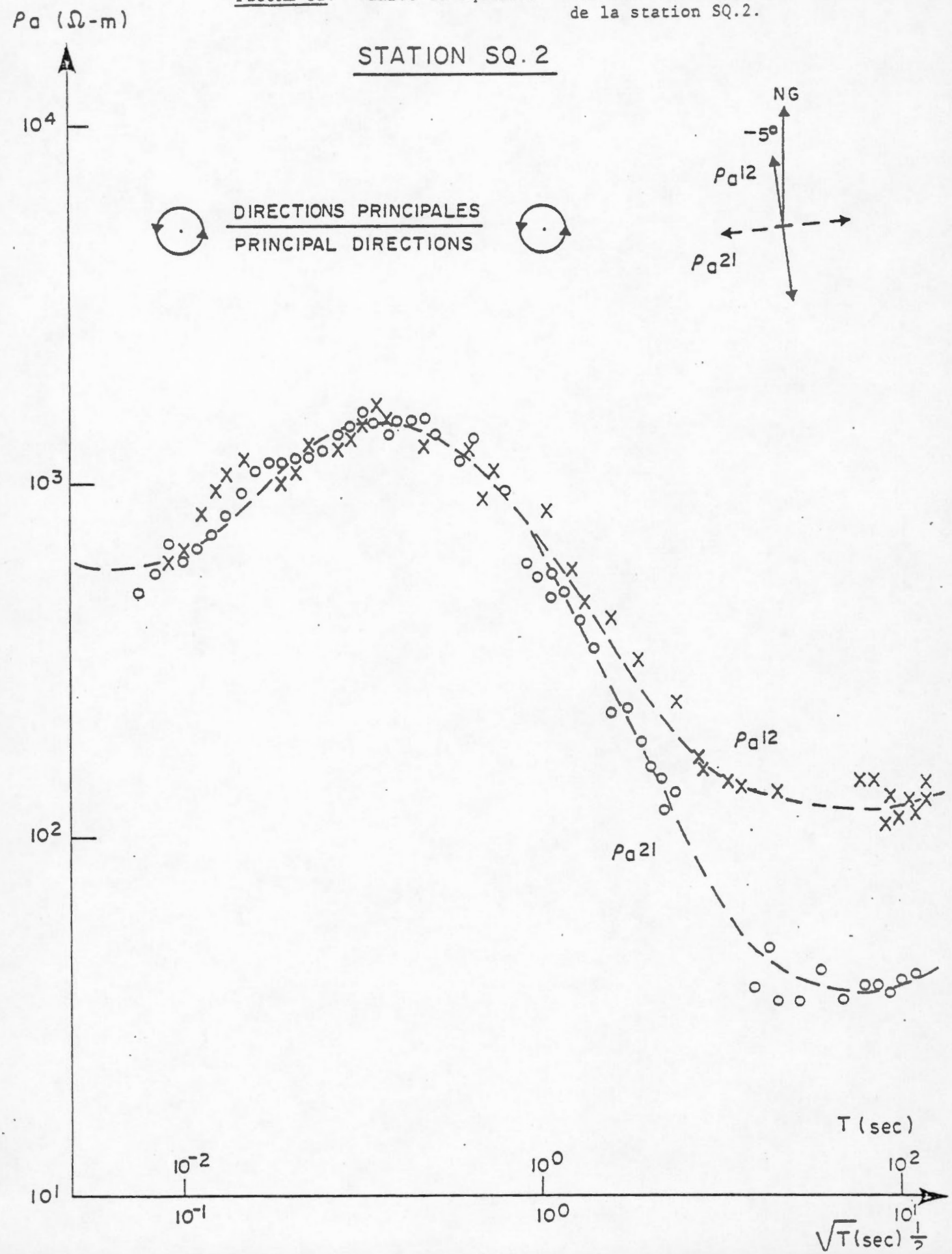

FIGURE 33. Vallée de Squamish - Courbes de sondage M.T. de la station SQ.3.

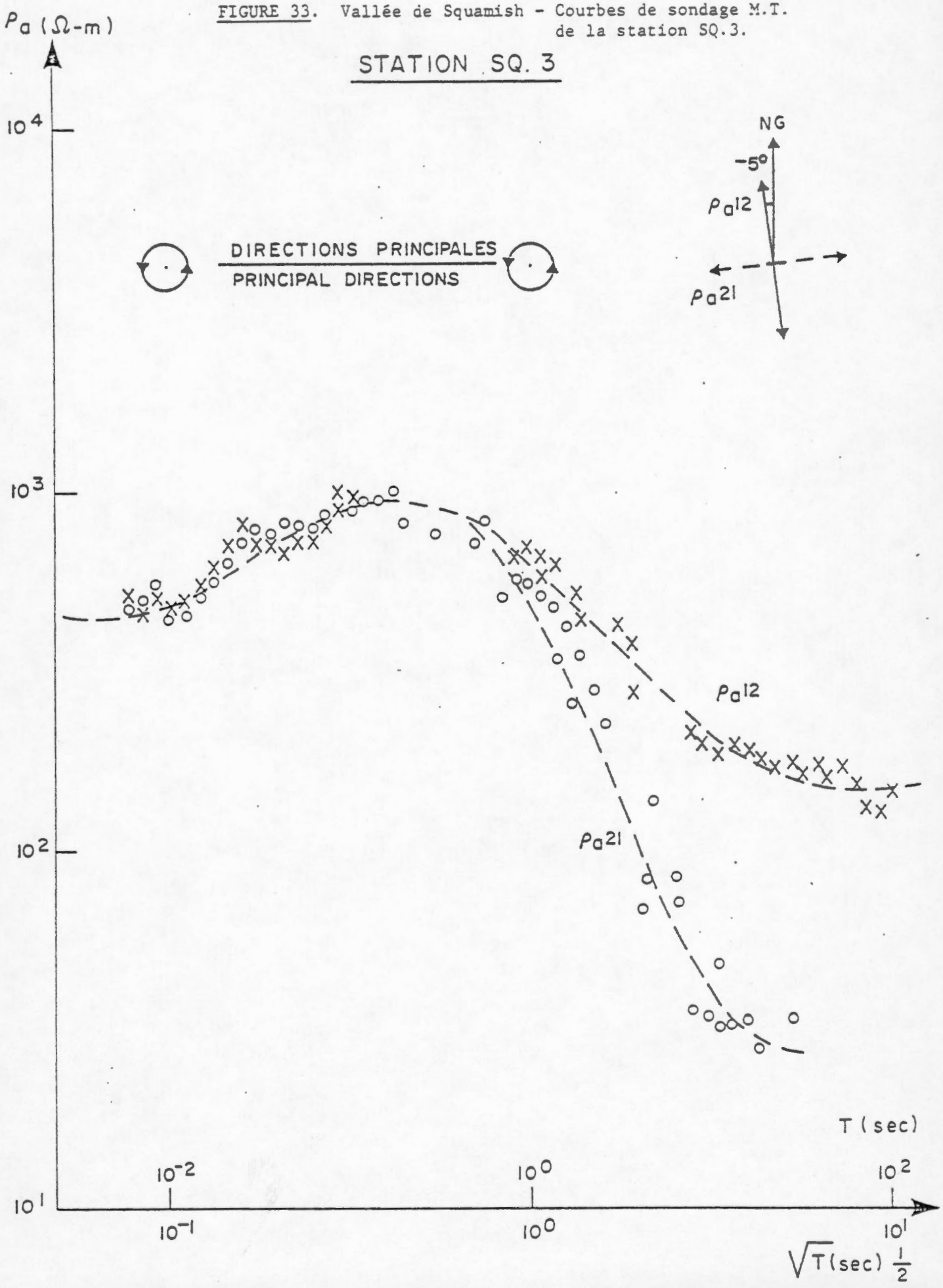

FIGURE 34. Vallée de Squamish - Courbes de sondage M.T. de la station SQ.4.

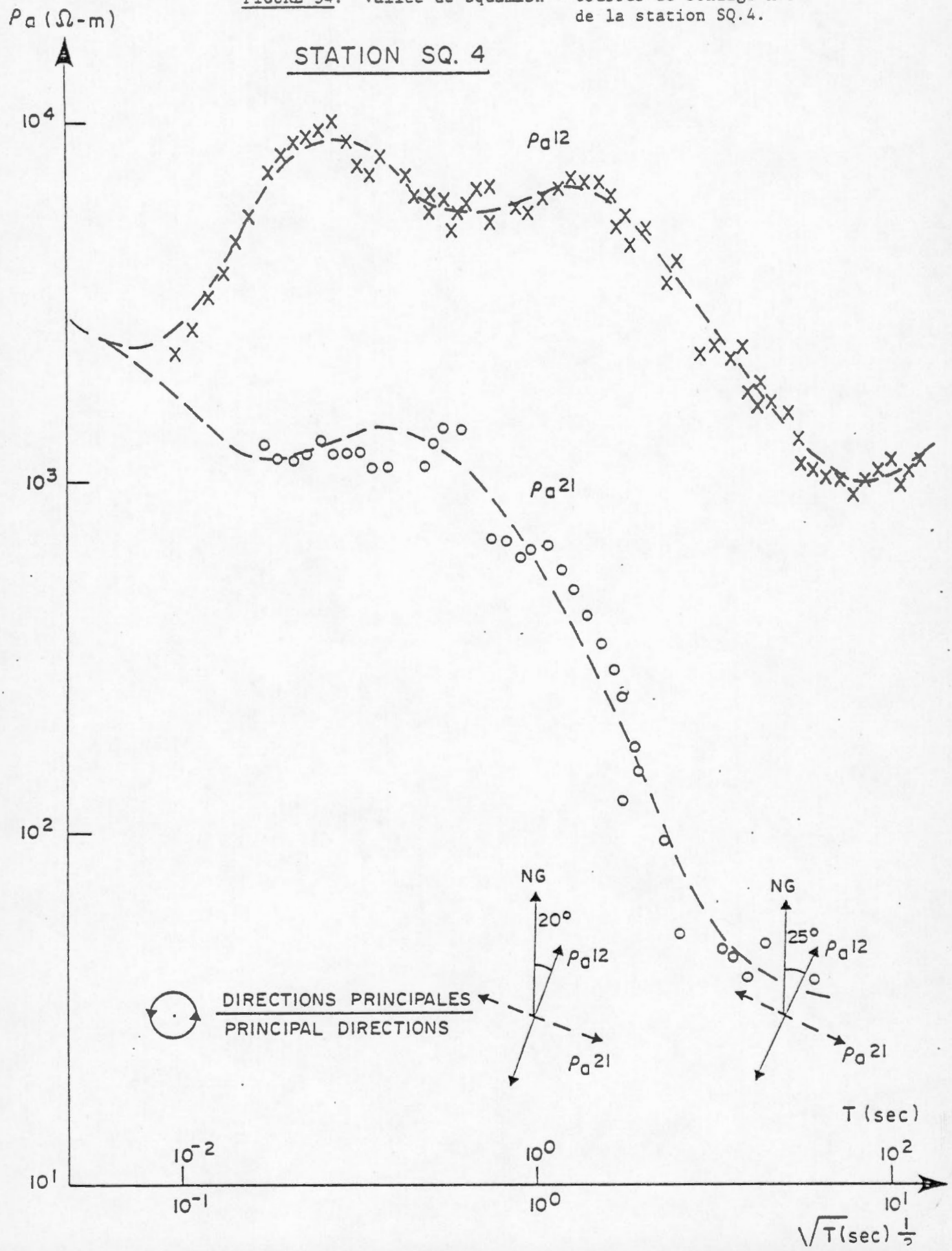

FIGURE 35. Vallée de Squamish - Courbes de sondage M.T. de la station SQ.5.

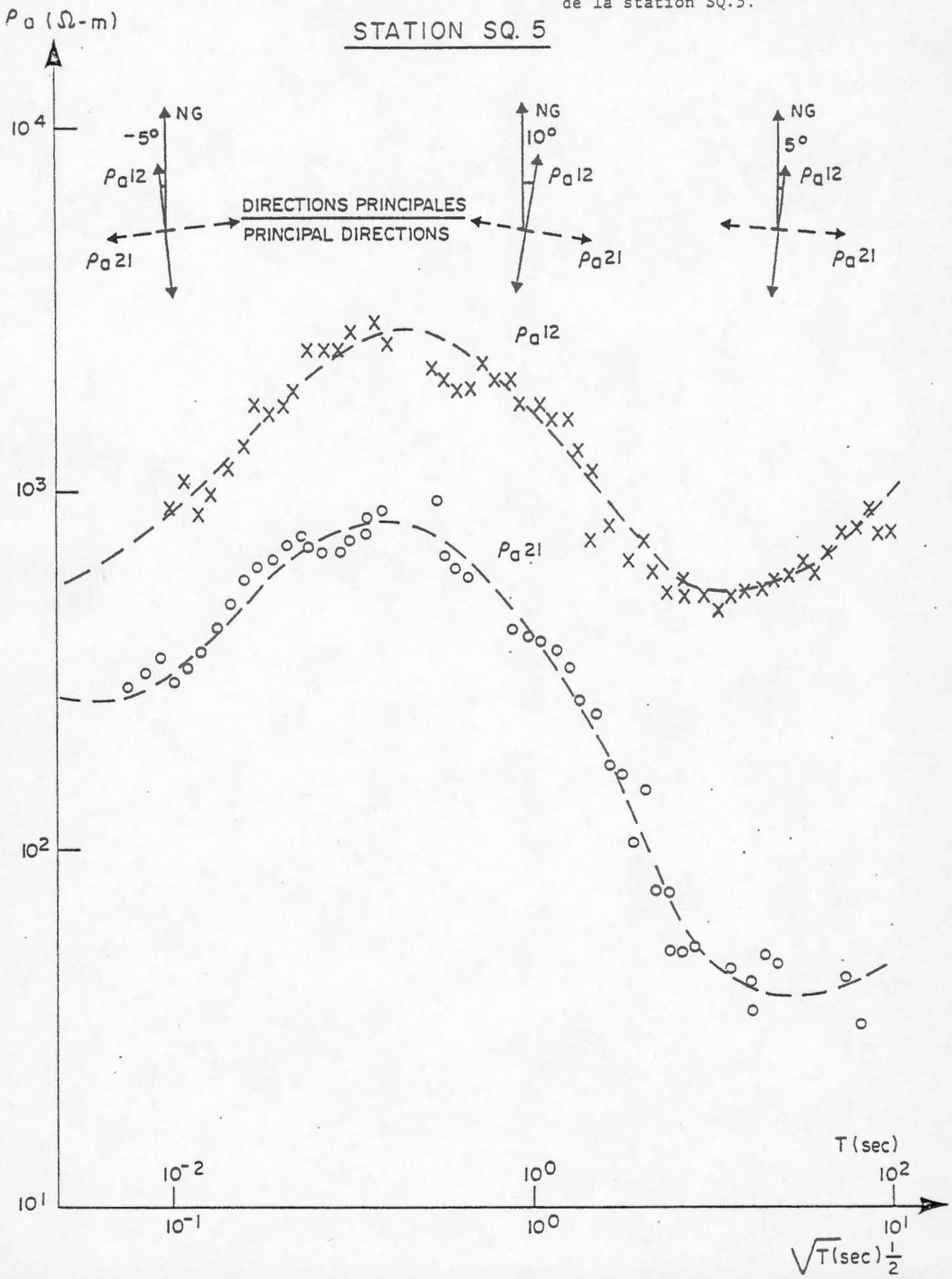

FIGURE 36. Vallée de Squamish - Courbes de sondage M.T. de la station SQ.6.

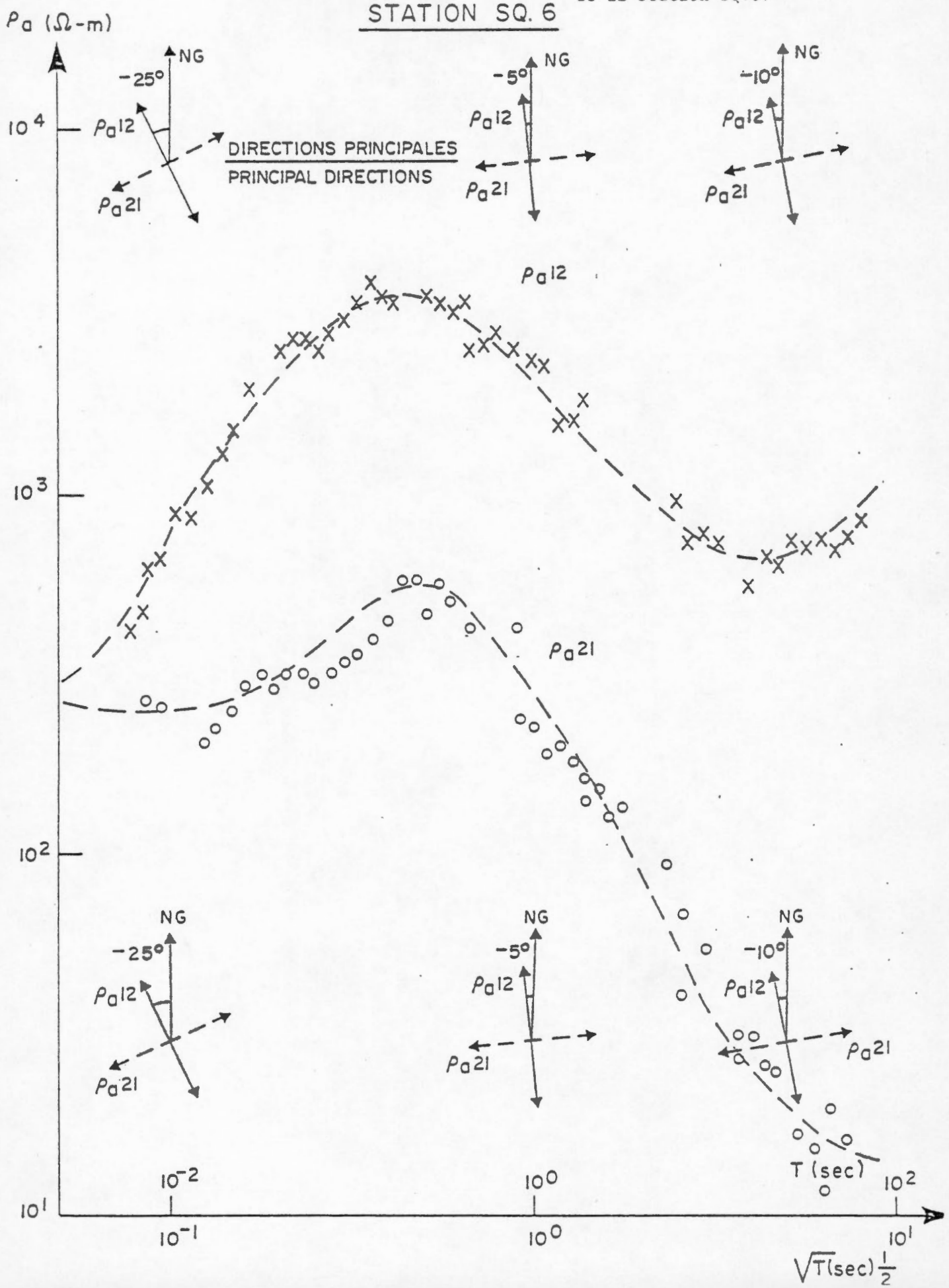

FIGURE 37. Vallée de Squamish - Courbes de sondage suivant la direction principale NS.

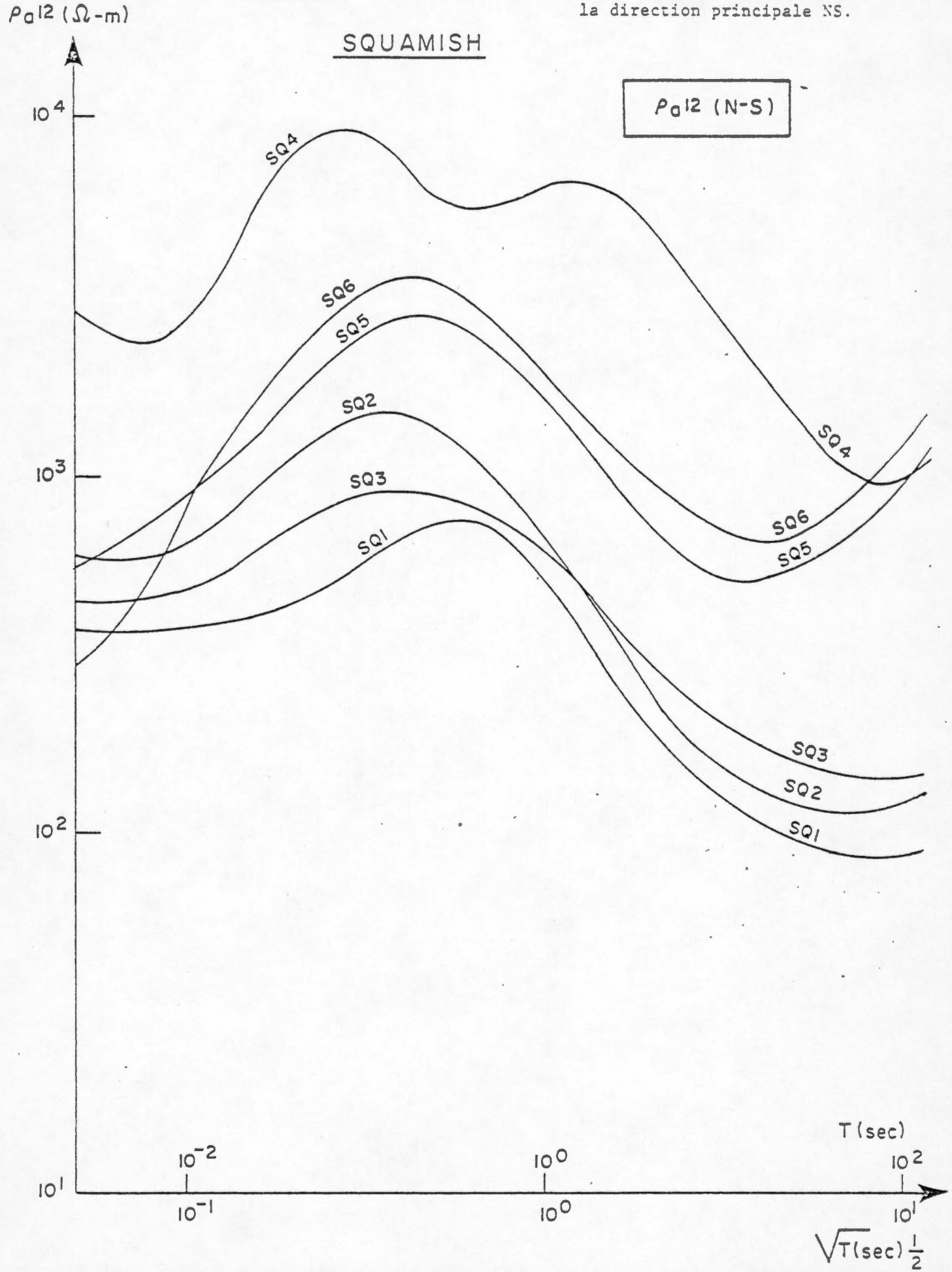

FIGURE 38. Vallée de Squamish - Courbes de sondage suivant la direction principale E-W.

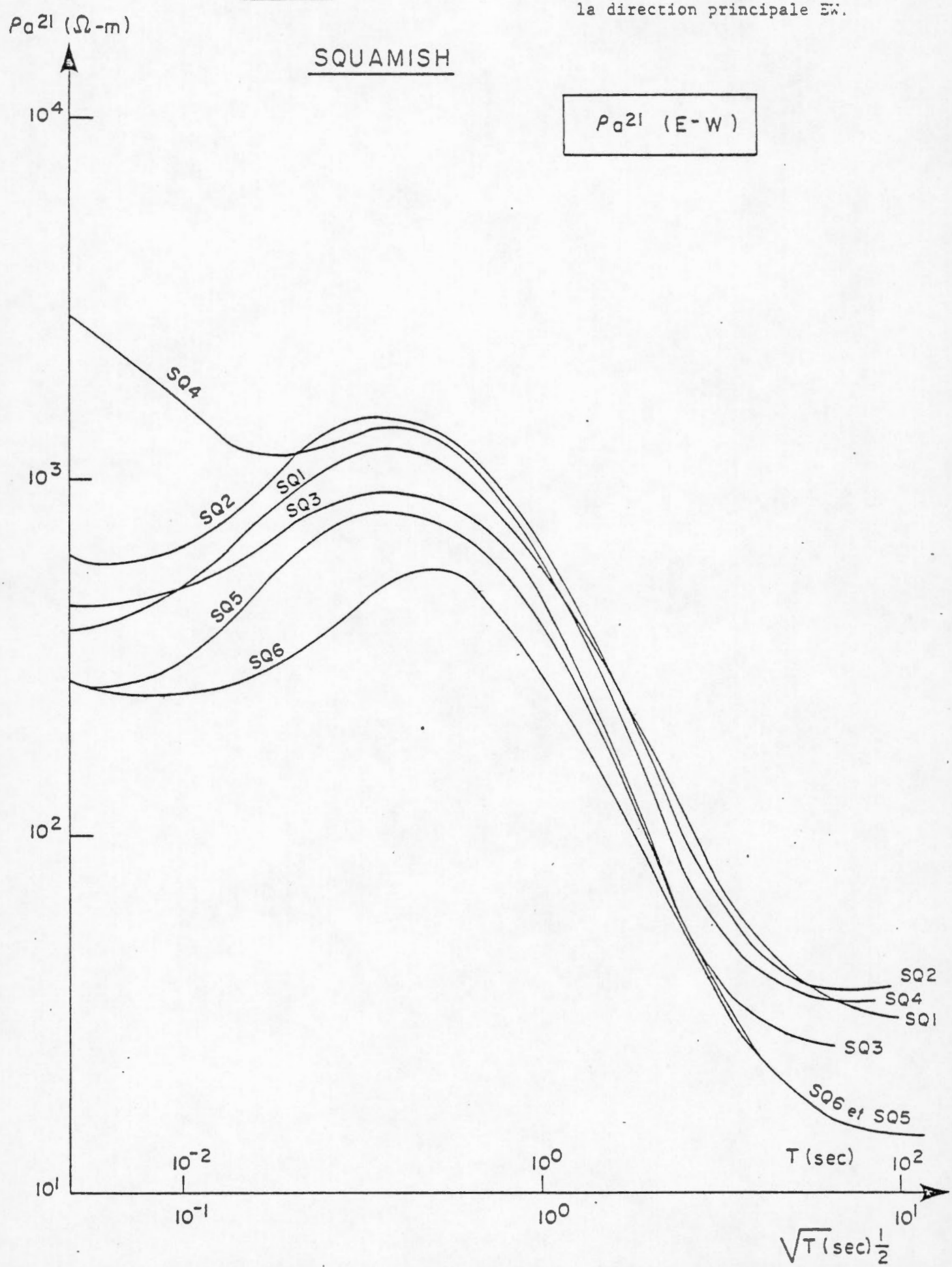

FIGURE 39. Vallée de Squamish - Interprétation par un modèle numérique à deux dimensions.

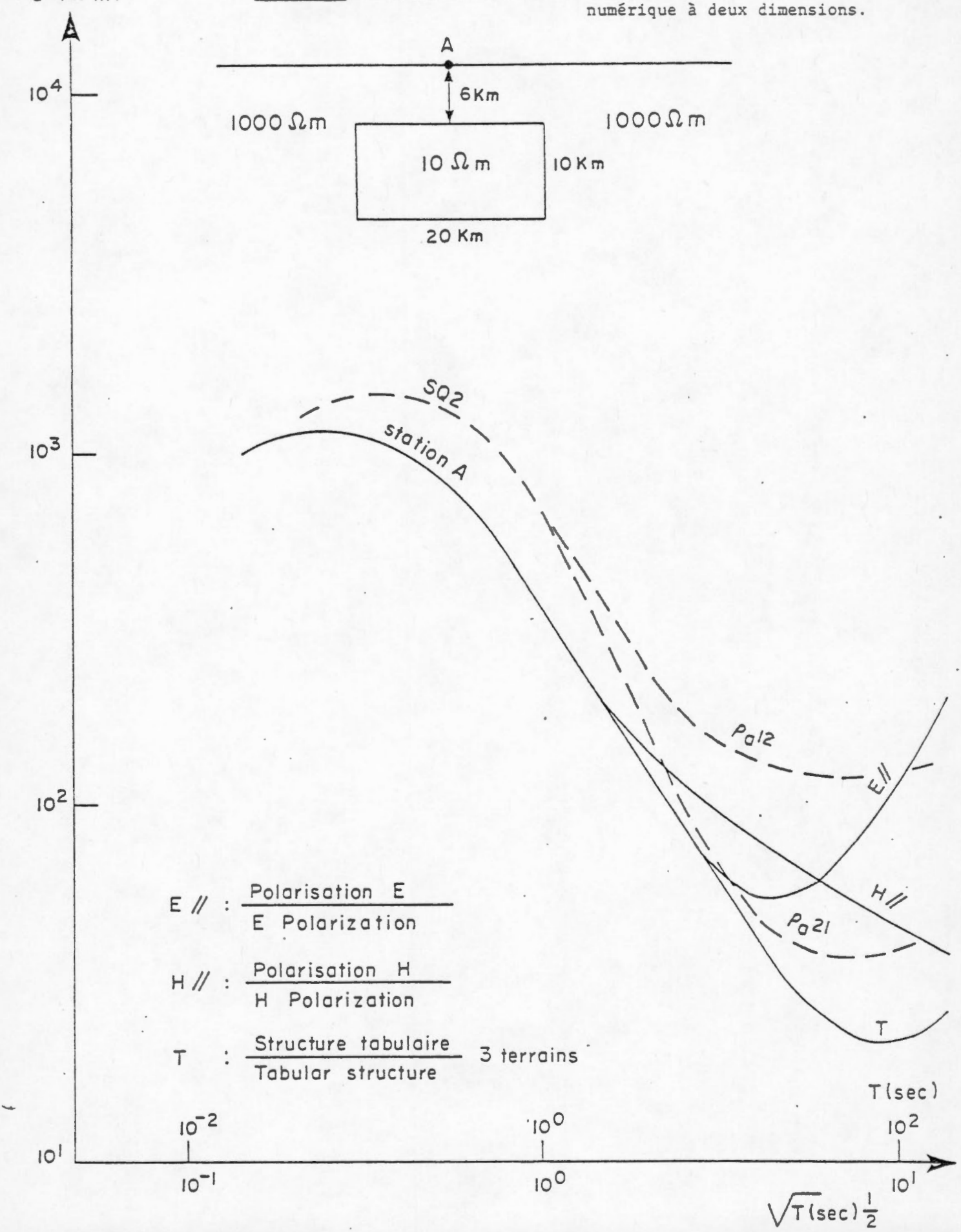

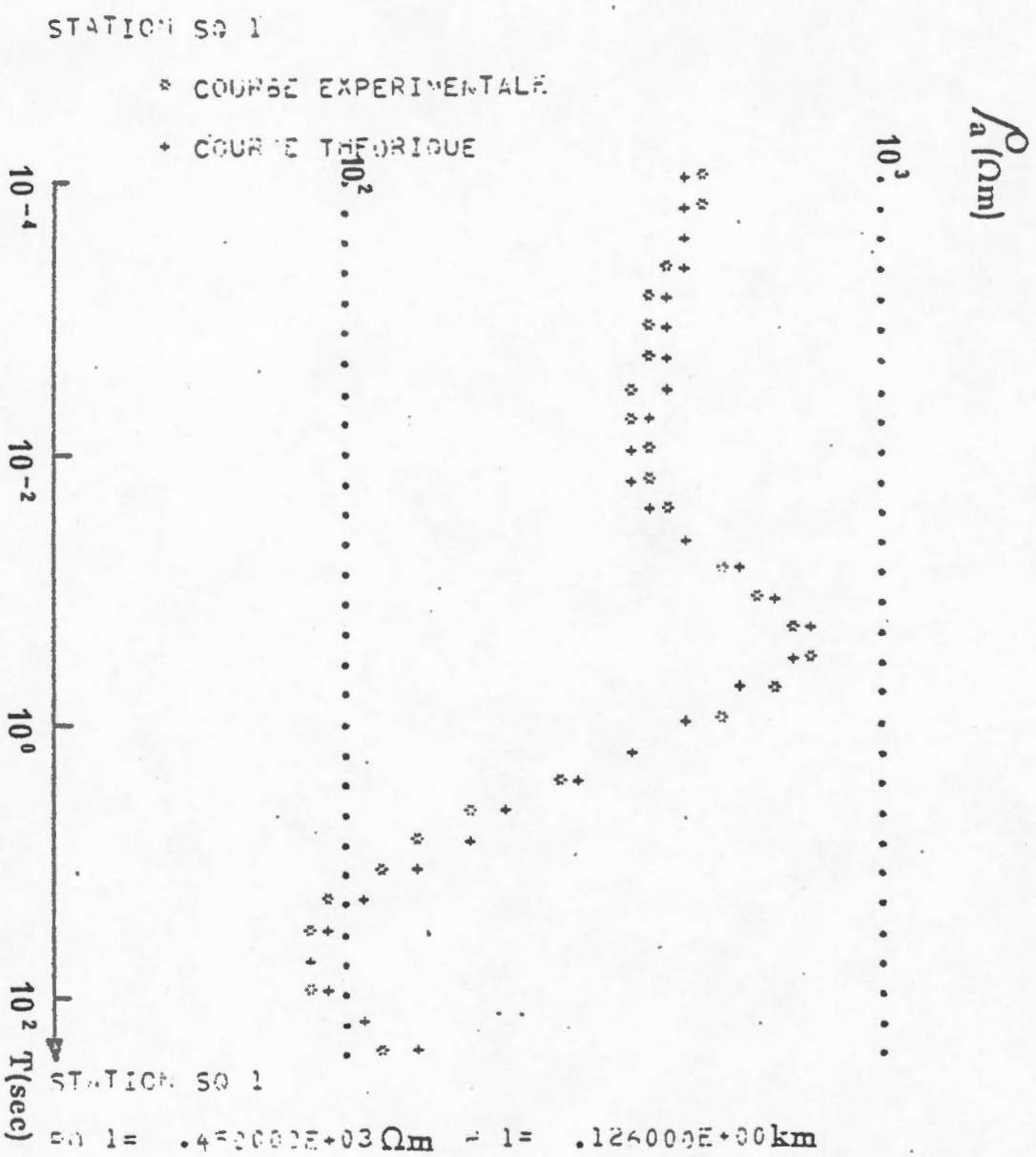

STATION SQ 1

RO 1= .450000E+03 Ωm H 1= .124000E+00 km

RO 2= .370000E+03 H 2= .120000E+01

RO 3= .130000E+04 H 3= .500000E-01

RO 4= .720000E+02 H 4= .300000E+02

RO 5= .100000E+04 H 5= ∞

FIGURE 40. Vallée de Squamish - Interprétation de la courbe $\rho_{a_{12}}$(NS) de la station SQ.1.

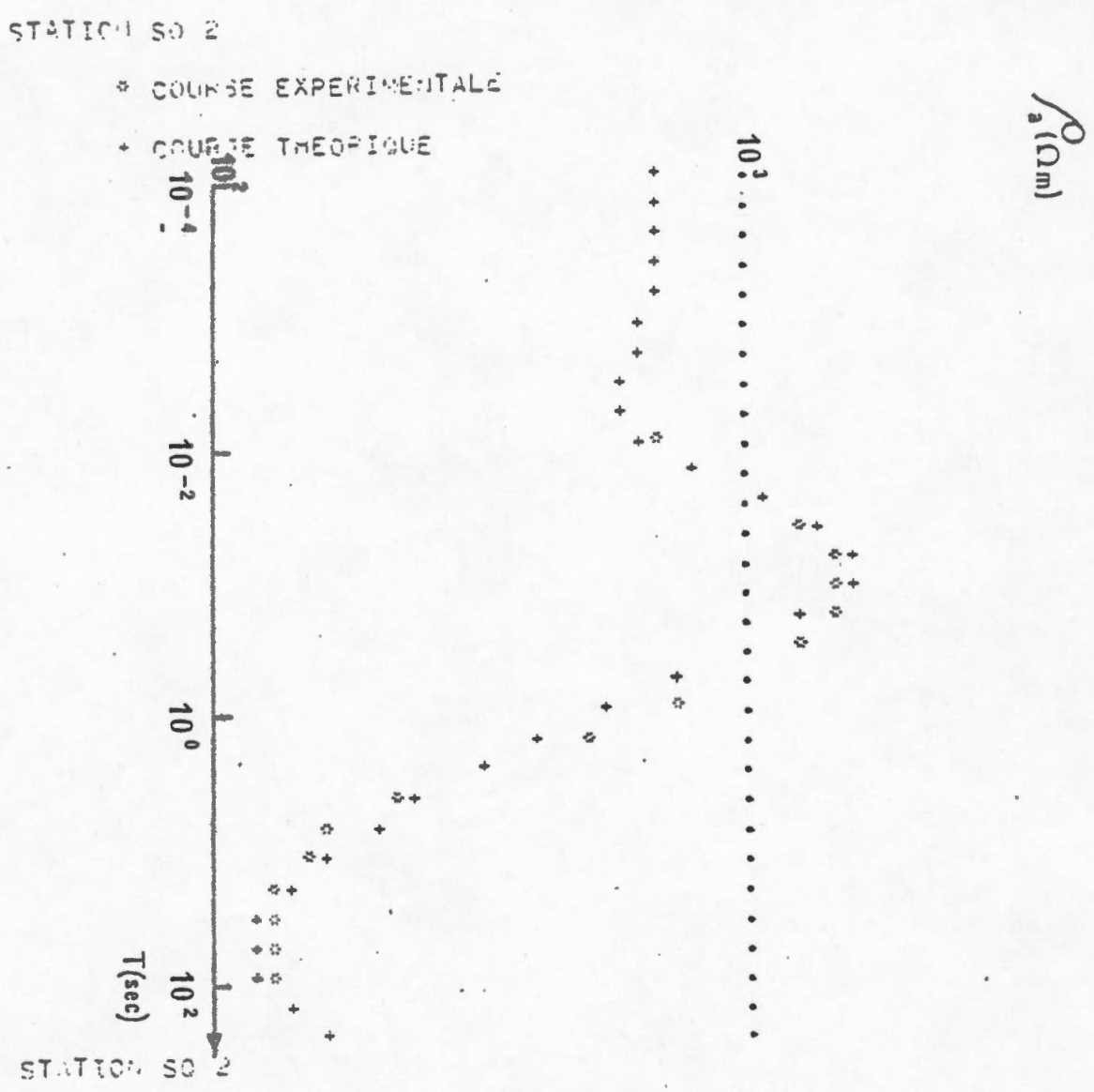

FIGURE 41. Vallée de Squamish - Interprétation de la courbe $\rho_{a_{12}}$(NS) de la station SQ.2.

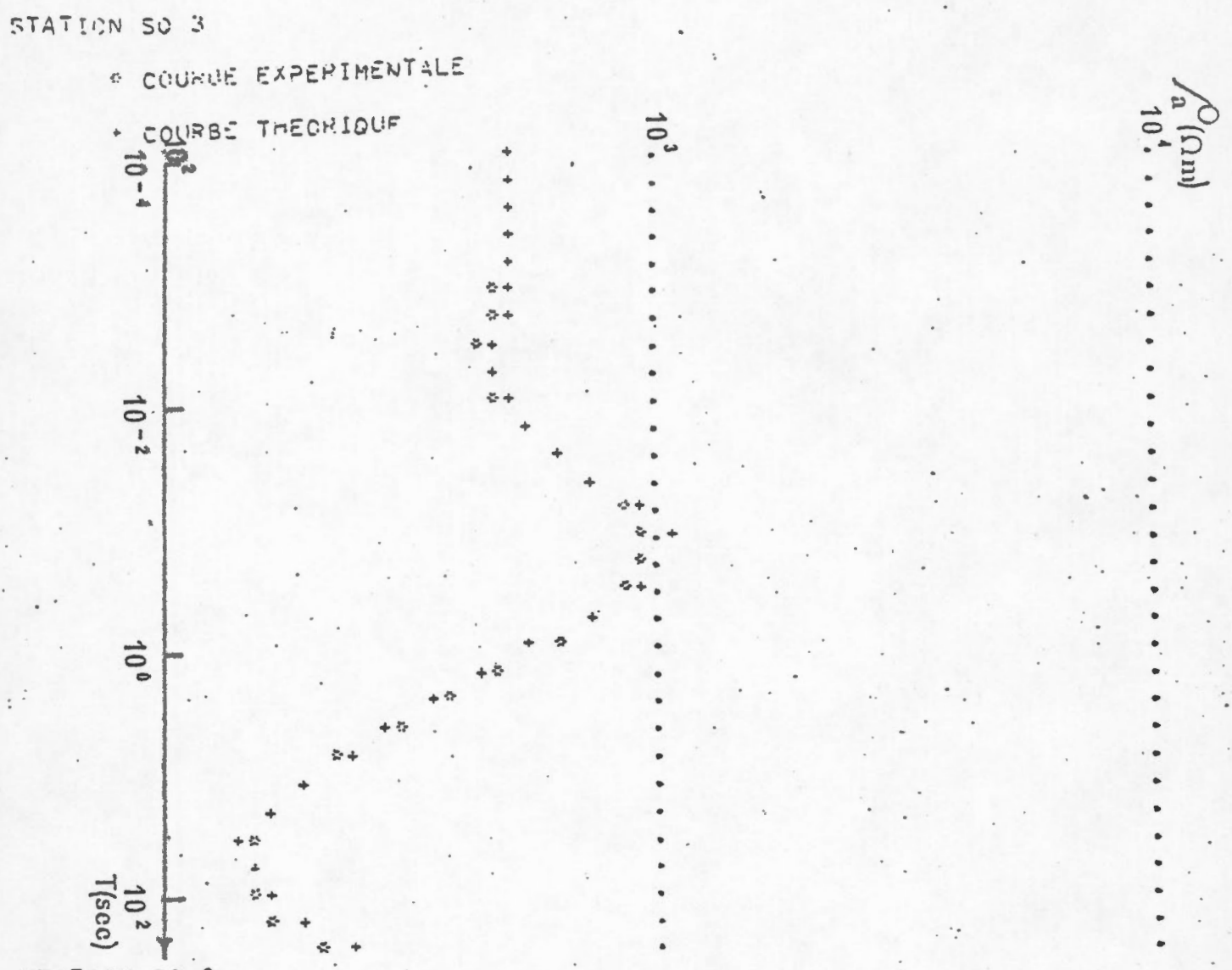

STATION SQ 3

RO 1= .500000E+03Ωm H 1= .950000E+00km

RO 2= .150000E+04 H 2= .550000E-01

RO 3= .110000E+03 H 3= .300000E+02

RO 4= .800000E+03 H 4= ∞

FIGURE 42. Vallée de Squamish - Interprétation de la courbe $\rho_{a_{12}}$(NS) de la station SQ.3.

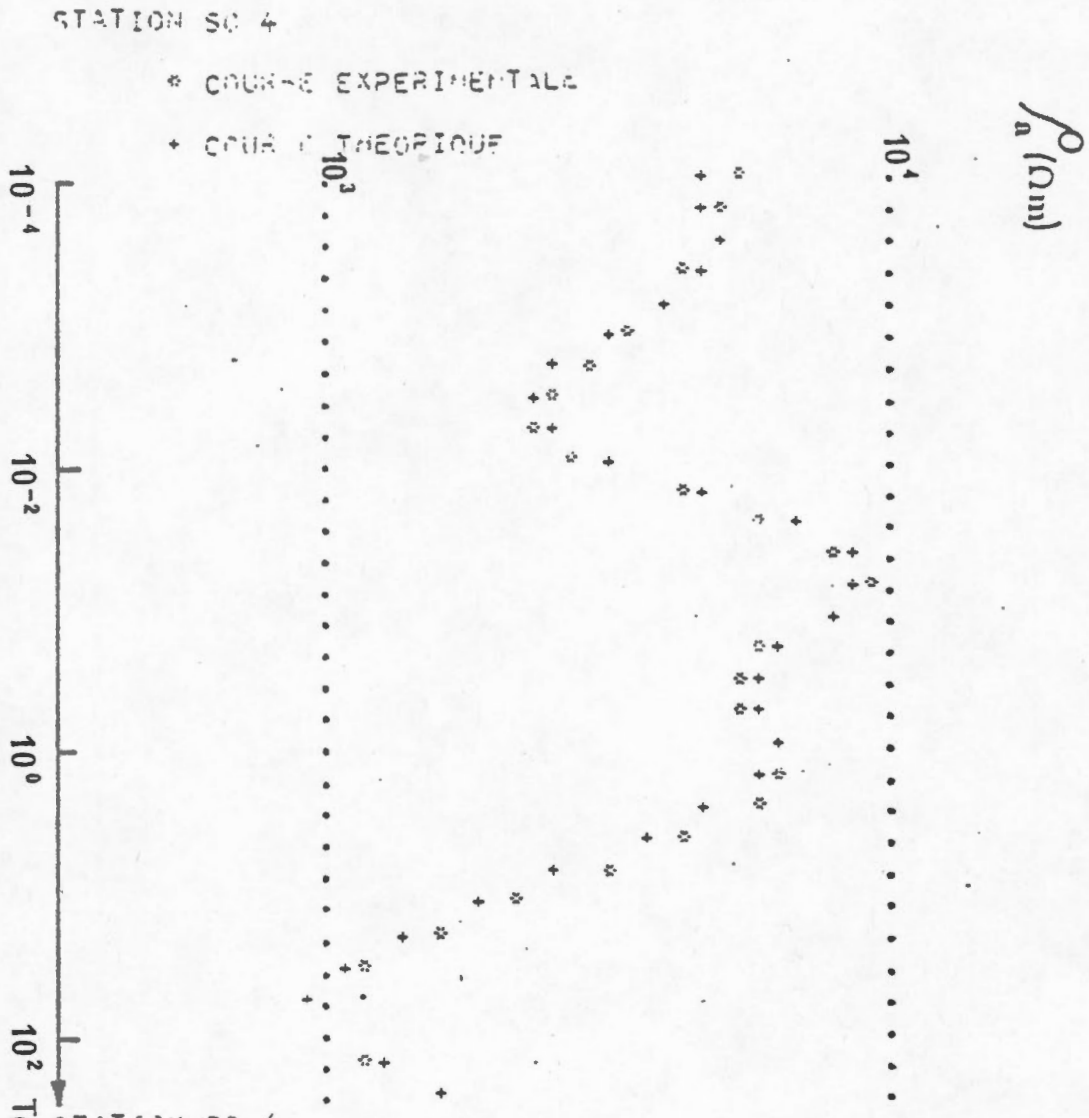

STATION SQ 4

ρ 1=	.[illegible]Ωm	h 1=	.650000E+00km
ρ 2=	.1070[illegible]	h 2=	.500000E+00
ρ 3=	.4[illegible]	h 3=	.120000E+02
ρ 4=	.6[illegible]	h 4=	.250000E+01
ρ 5=	.1[illegible]	h 5=	.250000E+02
ρ 6=	.[illegible]	h 6=	.450000E+02
ρ 7=	.1[illegible]	h 7=	∞

FIGURE 43. Vallée de Squamish - Interprétation de la courbe $\rho_{a_{12}}$ (NS) de la station SQ.4.

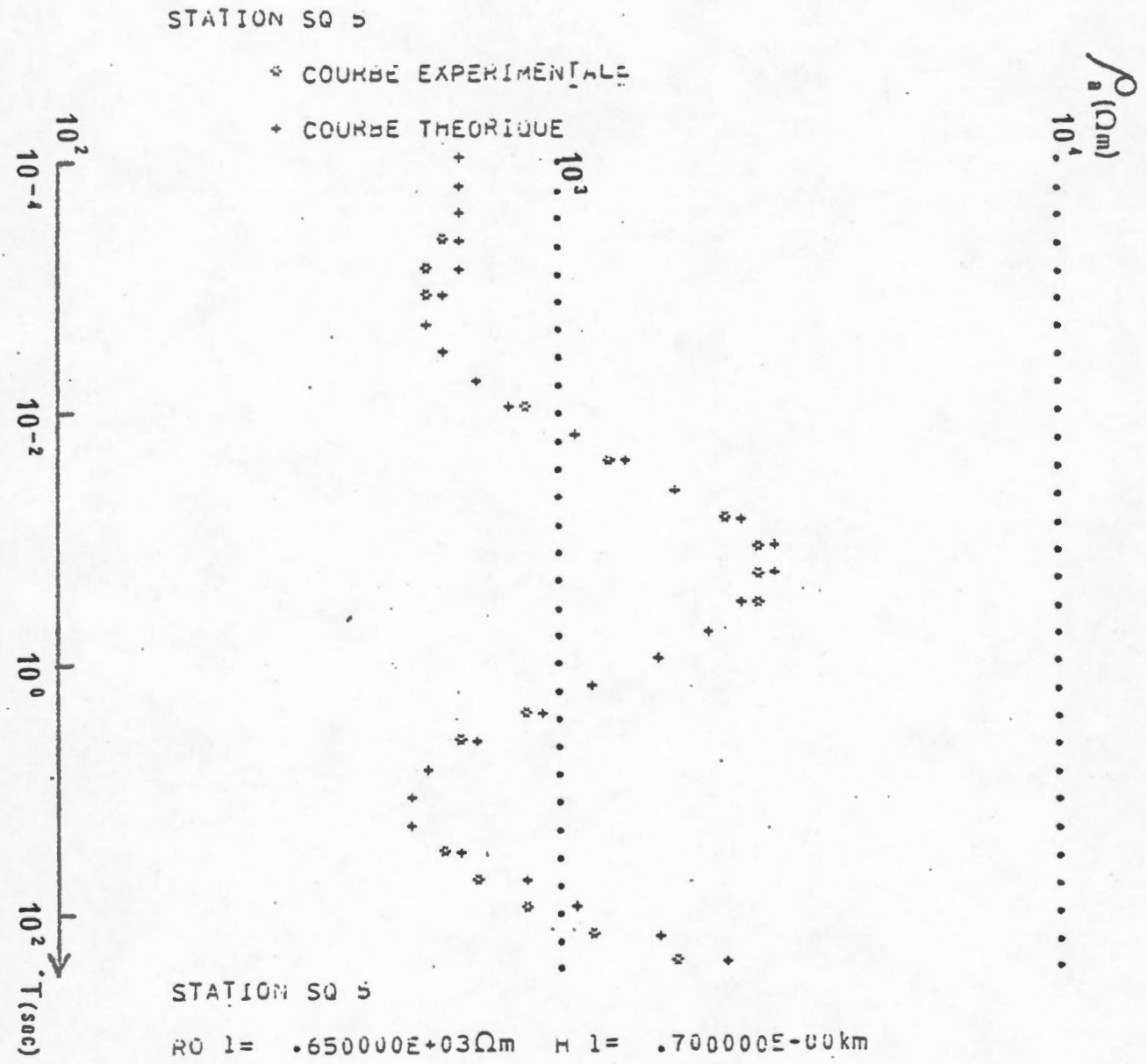

STATION SQ 5

RO 1= .650000E+03Ωm H 1= .700000E-00km

RO 2= .455000E+04 H 2= .100000E+0[illegible]

RO 3= .342000E+03 H 3= .2[illegible]0000E+0[illegible]

RO 4= .100000E+05 H 4= ∞

FIGURE 44. Vallée de Squamish - Interprétation de la courbe $\rho_{a_{12}}$(NS) de la station SQ.5.

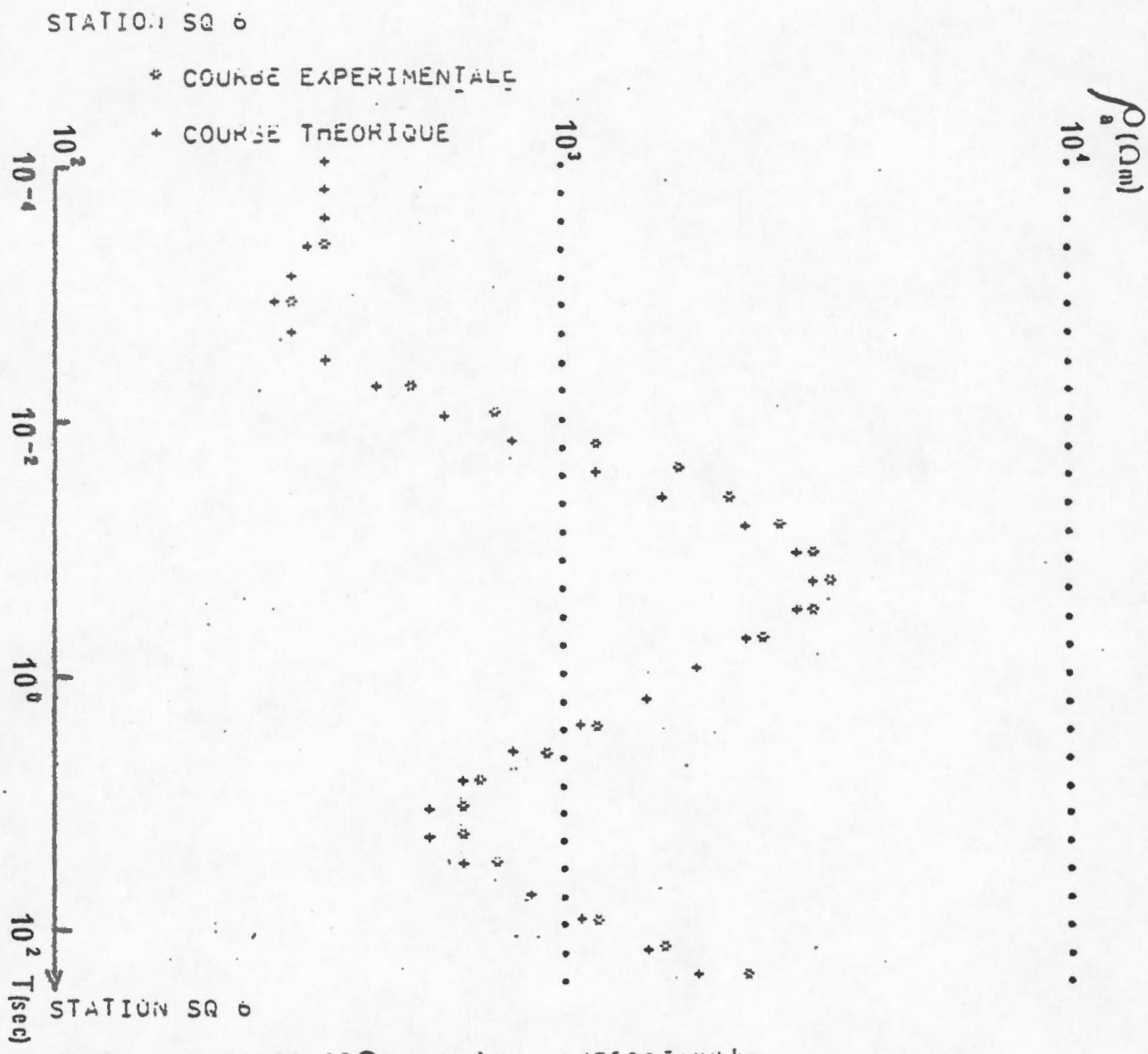

FIGURE 45. Vallée de Squamish - Interprétation de la courbe $\rho_{a_{12}}$ (NS) de la station SQ.6.

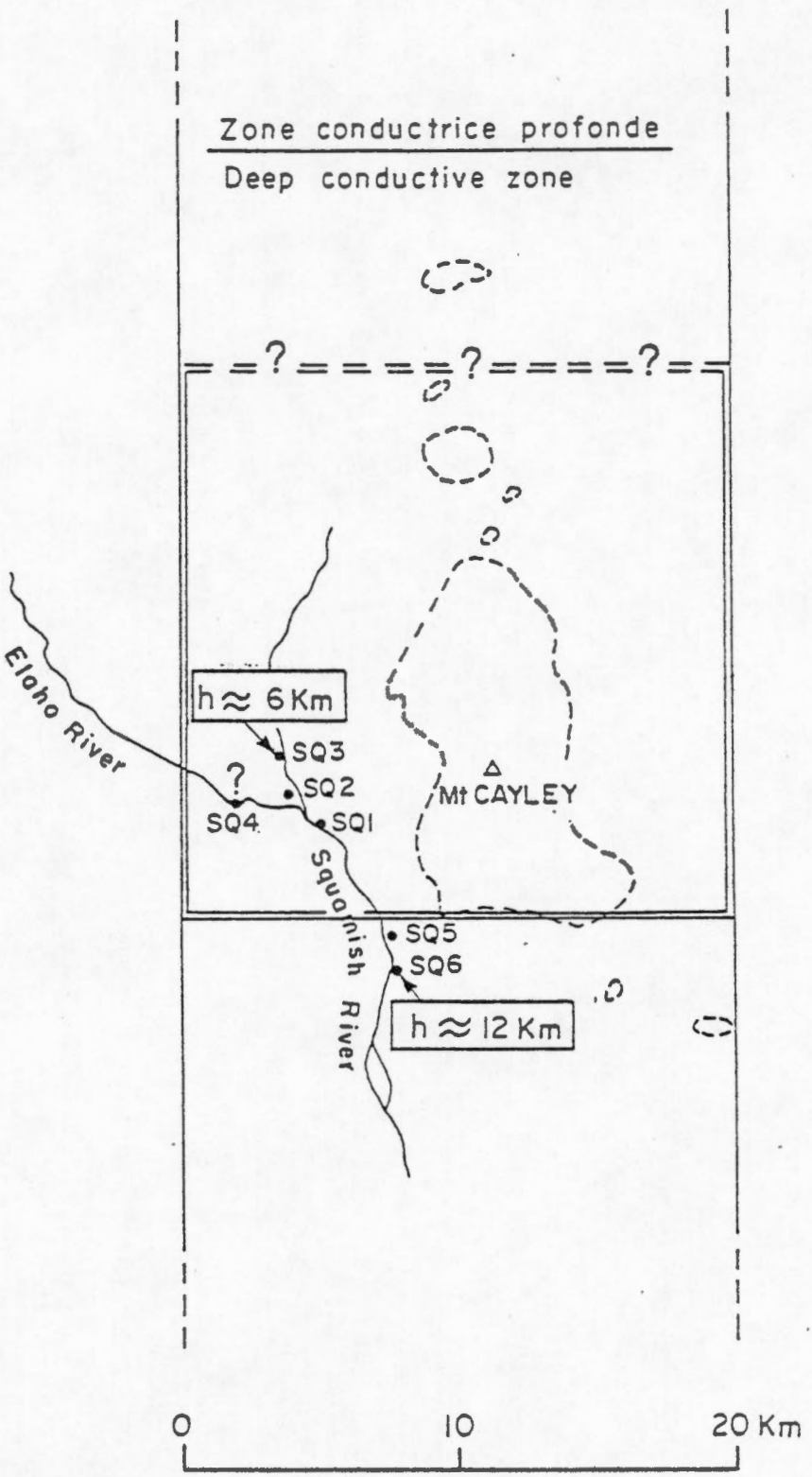

: Complexe volcanique du groupe garibaldi / Volcanic complex of the garibaldi group

h : Profondeur du toit de la zone conductrice / Depth of the top of the conductive zone

FIGURE 46. Vallée de Squamish - Hypothèse d'interprétation de la zone conductrice profonde.